Guideline for Optocoupler Ground Radiation Testing and Optocoupler Usage in the Space Radiation Environment

Guide for Optocoupler Ground Radiation Testing and Optocoupler Usage in the Space Radiation Environment

I. Introduction

Optocouplers (or optoisolators) are used in space and in commercial systems because they provide an efficient means of electrical isolation of microelectronic signals. Due to the non-space use of optocouplers, the numbers and types of these devices has proliferated. A recent check revealed that Agilent Technologies alone manufactures 55 different device types that use optocoupler technology—that is, they use light to provide electrical isolation. Optocouplers vary in design and functionality, and these differences can affect how the optocoupler responds to a radiation environment.

Assessing the risk of using optocouplers in satellite applications offers challenges that incorporate those of Commercial Off-The-Shelf (COTS) devices compounded by hybrid module construction techniques [LaBe-98]. We discuss approaches for estimating this risk for two types of optocouplers: 1) high bandwidth digital signal isolators, 2) those used to transfer current from one circuit to the next. Throughout this document when we use the word "optocoupler" we are generally referring back to these two optocoupler types.

This guide is intended to support insertion of these optocouplers into spaceflight applications and to recommend ground test protocols. The first guideline principle that should be followed is a serious concurrent engineering approach for down selecting space-qualified optocouplers. This requires that the design and component engineer seek the support of a radiation effects expert that understands Total Ionizing Dose (TID), Displacement Damage Dose (DDD) and Single Event Effects (SEEs) issue for optocouplers as applied to the system in question.

This guide is targeted towards two individuals: the design engineer and the radiation effects engineer. Rational will be provided for certain guidelines when this allows the radiation effects expert to assess applicability of the guideline for a specific mission and application scenario.

This guide assumes that the radiation effect expert has a working knowledge of the practices outlined in the four documents listed below. It uses terms and builds on procedures defined in these documents.

1. ASTM Guide F1192-00 - Standard Guide for the Measurement of Single Event Phenomena (SEP) Induced by Heavy Ion Irradiating of Semiconductor Devices [F1192]
2. JEDEC heavy ion testing guideline [JEDEC HI]
3. Proton test lesson learned document [p+ LL]
4. SET prediction tool for fiber links and optocouplers [MG]
5. ASTM Standard 883: Test Method 1019.5 [1019.5]

II. Optocoupler Technology

II.A Introduction

Optocouplers use a light emitter—typically a Light-Emitting Diode (LED)—to provide an internal optical signal to a photodetector and amplifier. The optocoupler provides a very high degree of isolation between the electrical signal that drives the LED and the output of the amplifier because there is no direct electrical connection between them (other than very small stray capacitance), only the optical signal. **Figure II.A.1** shows a block diagram of a typical optocoupler, which includes a LED and a photosector in a single package.

Past studies have shown that optocoupler performance is adversely affected by both radiation-induced permanent damage and SEEs [see for example: Rax- 96, Epst-72, Soda-75, Barn-84, D'Ord-97, LaBe-97, Reed-98, John-99b, LaBe-00, Reed-01]. Dealing with each of these effects poses its own specific set of challenges. The methods used to assess the risk to radiation-induced degradation depend heavily on the type of optocoupler and the application.

II.B *Optocoupler Types Addressed in This Guide*

The two classes of optocouplers we are addressing with this guideline are 1) current transfer optocouplers and 2) high bandwidth digital signal isolators. Each has special concerns when assessing the risk to radiation exposure.

Figure II.A.2 shows a typical current transfer optocoupler design. The optocoupler contains an emitter, transmission medium (not pictured), and receiver. The LED transmitter's function is to convert the electrical signal into an optical format. The role of transmission medium is to transfer the optical signal from the transmitter to the receiver. The optical receiver's purpose is to convert the optical signal launched into an electrical signal. The optical signal is detected by the phototransistor, its output current is related to the intensity of the optical signal.

Figure II.A.3 shows a typical design for a high bandwidth digital signal isolator. Like the current transfer optocoupler, these types of couplers have an emitter, transmission medium (not shown) and a receiver. However, in this case the receiver is a photodiode followed by an amplification circuit.

II.C Construction Techniques

Figure II.A.4 shows two different construction techniques for optocouplers. Optocouplers are very simple hybrid devices, consisting of an LED assembly, mounted on a carrier, with a silicon integrated circuit containing a photodiode and transistor (or high-speed amplifier). Some manufacturers produce only the photodiode/amplifier, purchasing the LED from outside sources, while others fabricate and control the LED as well as the silicon-based portion of the optocoupler.

Different physical configurations are used to fabricate optocouplers. Direct coupling, shown in **Figure II.A.4(a),** uses a surface-emitting LED that is inverted and placed directly over the photodetector in the silicon die. This approach is straightforward, providing highly efficient light coupling. A thin layer of optical coupling material (barely detectable in the figure) is usually placed between the LED and photodetector in order to reduce Fresnel losses. This method is often used for high bandwidth digital signal isolators.

As opposed to the direct method, the indirect method, shown in **Figure II.A.4(b)**, uses a side-emitting LED. It relies on total internal reflection from a silicone compound that is placed over the LED and detector/amplifier. Optocouplers with indirect coupling are easier to fabricate compared to those with the direct coupling method shown in **Figure II.A.4(a)**. However, the amount of light that is transmitted depends on physical properties that are difficult to control— the roughness of the cleaved edge of the LED and the presence of bubbles in the silicone as well as on the electrical properties and optical efficiency of the two materials. Many optocouplers are made with indirect coupling because of the ease of manufacturing them along with improved voltage isolation between the LED assembly and the silicon subassembly compared to optocouplers with direct coupling. The indirect method is typically used for current transfer isolators.

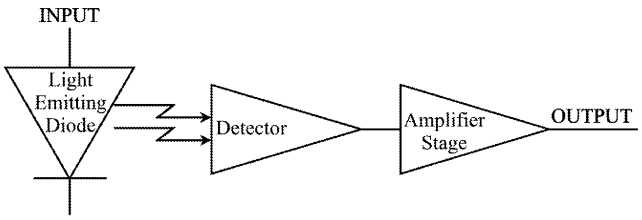

Figure II.A.1
Representative optocoupler design. The receiver side contains a detector and possibly a simple amplification stage [Reed-98].

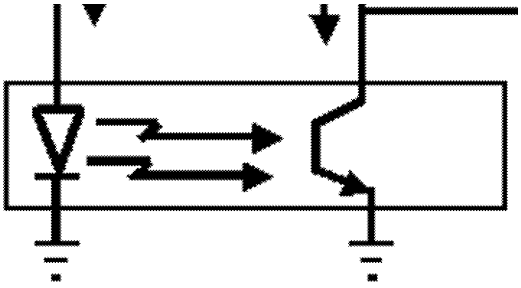

Figure II.A.2
Typical current transfer optocoupler design

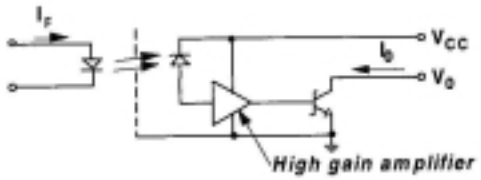

Figure II.A.3
Typical high bandwidth digital signal isolators design [John-99b].

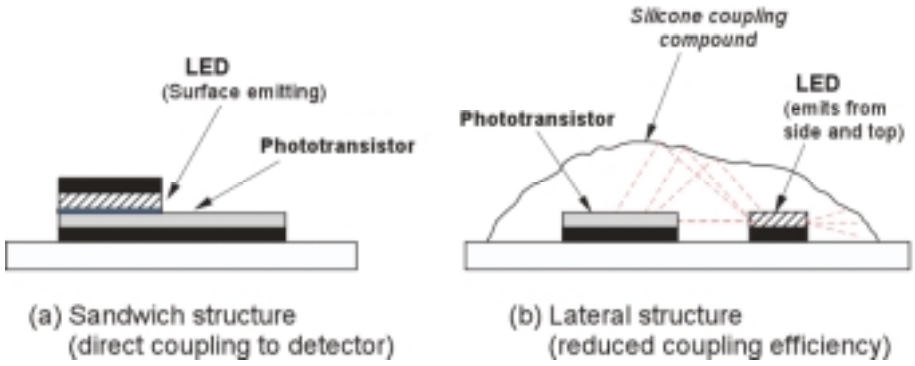

Figure II.A.4
Diagram of two basic optocoupler configurations [John-00].

III. Radiation Induced Failure Mechanisms in Optocouplers

III.A Introduction to Basic Radiation Effects

The components that make up an optocoupler rely on such carefully grown, well-defined microscopic structures that can have very low tolerance for slight changes in their characteristics. When a component is exposed to radiation, the radiation transfers some of its energy to the component materials, changing the

localized material properties. This can have significant effects on component functionality and/or parametrics with the end result depending on the type of radiation and where within the optocoupler the energy deposition occurred.

In this section we will review the SEEs, TID and DDD effects that occur when a optocoupler is exposed to radiation, **Table III.A.1** list components used to makeup optocouplers and the performance degradation mechanisms that are most important for each. We will briefly consider these radiation effects and how these effects may degrade optocoupler performance. We will first consider single-event transients in photodetectors and amplification circuitry. Next, we will consider permanent degradation of optocoupler parametrics.

Table III.A.1
Dominate performance degradation mechanism for each component of an optocoupler.

LED	DDD
Photodetector	TID, SET
Amplification Circuit	TID, SET
Coupling Medium	TID

III.B Single-Event Transients

An ionizing particle generates electron-hole pairs along its path as it passes through a material, resulting initially in a line charge distribution with equal numbers of holes and electrons. Because the function of active optocoupler components is governed by the controlled injection of charge into the depletion layers of p-n junctions, the uncontrolled charge injection resulting from ionization can produce a self-recoverable false-signal on the output of the optocoupler. These false signals are know as Single Event Transients (SETs). Particles incident on the photodetector or amplification circuitry can produce SETs, the photodetector is typically much more sensitive.

Generally, the variable of choice used to characterize heavy ion induced SETs is Linear Energy Transfer (LET), which is the negative of the energy deposited per unit path length (-dE/dx) normalized to the medium's density (-1/ρ*dE/dx) expressed in MeV*cm^2/mg [Zieg-84]. This is known as Direct Ionization. In general, the higher a particle's LET—or, equivalently, the denser its charge track—the higher the probability that it will cause an SET. The probability of an SET to occur is expressed as a cross-section (number of events divided by the particle fluence), with dimensions appropriate to the device (μm^2 or cm^2). Eventually, the cross-section will become saturated at some LET, i.e. increasing LET has no effect on cross-section.

Proton induced SETs in high speed optocouplers were reported first by LaBel, et al. following an investigation onboard flight anomalies due to single particle event effects in optocouplers used on the Hubble Space Telescope (HST) [LaBe-97]. Protons can generate ionization by either direct means—in which the proton, itself generates the charge—or by indirect means—in which the products of a proton-nucleus collision generate the charge. Either of these event types can induced an SET at the output of an optocoupler. For most microelectronics, proton direct ionization generates far too little charge to be an SEE concern. However, the high sensitivity of some photodetectors contained in optocouplers means that proton direct ionization cannot be ignored. **Figure III.B.1** shows, in pictorial form, the fact that both direct and indirect ionization can induce an SET on the output of an optocoupler. The long pathlength through the photodetector at grazing angles plays a critical role for the case of direct ionization. This has significant testing implications that will be discussed later.

Figure III.B.2 demonstrates this result for the photodetector in an optocoupler. As can be seen, the SET cross-section for protons at near-grazing incidence (90 degrees on this chart) is more than an order of magnitude higher than the cross-section for normally incident protons—this despite the fact that the physical device cross-section is actually lower for grazing-incidence protons. This result has been interpreted as an indication that for sufficiently long path lengths within the detector, even protons can directly generate enough ionization to cause SETs [LaBe-97]. A consequence of the increase in grazing-angle cross-section is that in proton-rich environments, proton-induced SET rates may dominate versus those caused by heavier ions and by indirect ionization [LaBe-97].

Figure III.B.3 shows an example of the increase in SET cross-section with the incident angle for the Agilent HCPL5231 optocoupler for three different proton energies. At 60 MeV, the angular dependence is very weak, but for the lower energies the effect stronger. For 42 MeV protons, the cross-section at grazing incidence is a factor of 10 higher than the cross-section at normal incidence. For 31 MeV protons, the grazing incidence cross-section increases by nearly two orders of magnitude. This dependence indicates that transients caused by direct ionization by protons traversing the diameter of the photodiode dominate at grazing incidence [Reed-01].

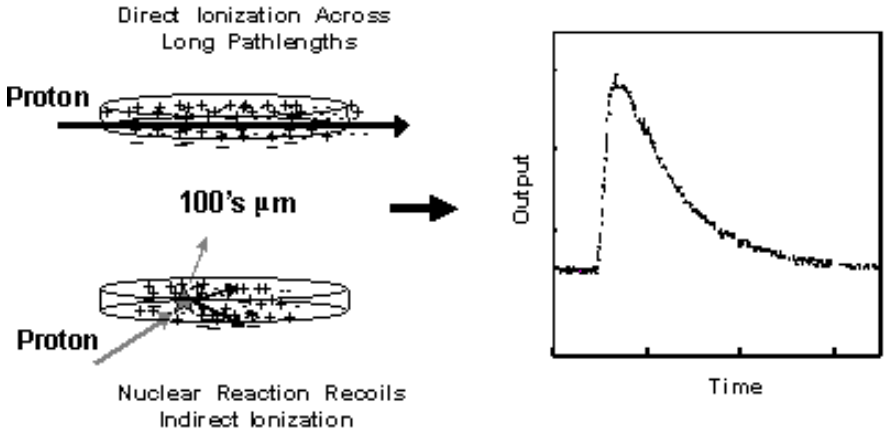

Figure III.B.1
Protons can generate charge in a device by either direct or indirect ionization. If sufficient ionization is generated, a single-event transient (SET) may result. [Adapted from LaBe-97].

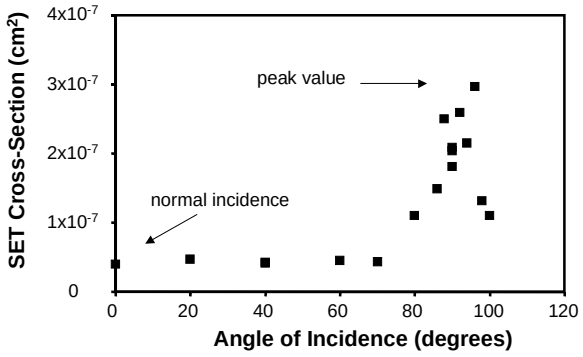

Figure III.B.2
The SET cross-section for protons incident on a photodiode increases dramatically as the protons approach grazing incidence—an indication that direct ionization is becoming important [LaBe-97].

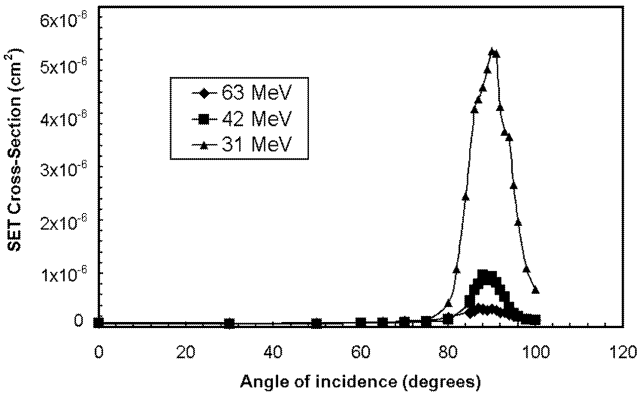

Figure III.B.3
Effect of incident angle on cross-section of the Agilent HCPL5231 optocoupler for various proton energies [Reed-01].

The photodetector is not the only component sensitive to SET. Particle strikes in the high gain amplifier can also produce SETs on the output. These SETs add to those associated with the photodetector to give the total SET cross-section [John-98]. Amplifier circuits sensitivity to radiation is described by the classical response curves, i.e., these circuits are not sensitive to direction ionization effects when exposed to protons.

Finally, low bandwidth current transfer devices can be sensitive to SETs, however these device have critical charges or bandwidths such that the proton direct ionization is too low to induce an effect. **Figure III.B.4** shows heavy ion induce SET cross-section for HP 6N140 [John-98]. These types of data are similar to the classical data taken on many electronic devices. The established methods for assessing the on-orbit event rate may be used to assess the performance of the optocoupler when used in space flight. A much more difficult case is when the optocouplers are sensitive to proton-induced direct ionization effects.

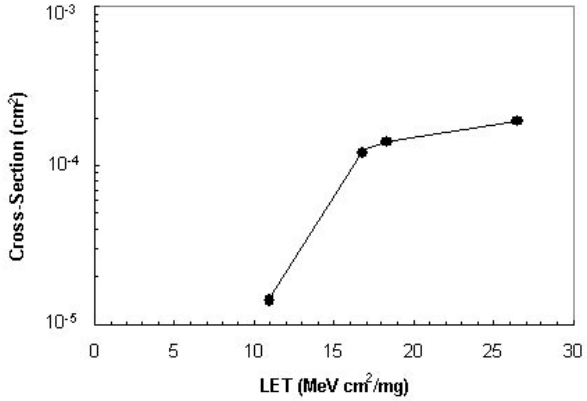

Figure III.B.4
Cross-Section versus LET for the HP 6N140 [John-98].

III.C Permanent Degradation

Damage from TID is caused by the electron-hole pairs generated by ionizing radiation that passes through a material. These charges can gradually change the performance of an optocoupler component, with the level of change depending on the total ionizing energy absorbed—that is, on the TID [Dres-98, Lera-99, and references given in these]. Generally, TID changes the characteristics of the materials that make up a component, resulting in gradual parametric degradation and changes in functionality. In most cases, the basic cause of TID degradation is the trapping of charge in a medium, e.g., a field oxide or in an optical medium.

DDD, on the other hand, has a different damage mechanism. The proper functioning of active optocoupler components depends critically on the semiconductor having a pristine crystalline lattice. However, this lattice can be damaged when an energetic particle, such as a neutron, electron, proton or heavy ion displaces one or more nuclei within the crystalline lattice, creating electrically active defects. As this damage to the crystalline lattice—called the displacement damage—increases, the device can degrade parametrically, and eventually stop functioning all together. For the most part, because protons are penetrating, strongly interacting and abundant, the proton environment is predominant in considerations of DDD effects in shielded applications. The 1999 Nuclear and Space Radiation Effects Conference (NSREC) Short Course [Mars-99] explores DDD effects in further detail.

What follows in this section is a brief description of DDD effects in LEDs, effects of TID on the passive transmission media, and finally an examination of the effects of TID and DDD of the photodetectors and amplification circuit.

III.C.1 Permanent Degradation in LEDs

The role of LEDs in an optocoupler is to convert current signals into light. For these devices, we are generally more concerned with permanent degradation due to DDD. TID is often a second order effect [Barn-84, Barn-86, Mars-92]. Also, because the drive signals for these devices are usually on the order of milliamperes, the small currents generated by ionizing radiation (usually picoamperes) are insufficient to cause SETs.

LEDs produce light by means of radiative recombination of injected minority charge carriers with majority carriers in the depletion region. As such, any damage that decreases the efficiency of radiative recombination or introduces competing processes will degrade device performance. Irradiation by heavy particles such as protons and neutrons can displace nuclei from the crystalline lattice, causing DDD. These defects can serve as sites for nonradiative recombination, decreasing the efficiency of the light source [Barn-84]. See [John-00] for a detailed discussion on DDD effects in LEDs.

Displacement damage decreases the LED output power, which in turn can reduce the output current of the photodetector. For current transfer applications, this results in a decrease in the device output current eventually leading to device failure. For data transfer applications, this will result in device inability to transmit data.

III.C.2 TID Degradation of Transmission Media

Although charged particles traversing an optical medium can generate photons, these processes are too weak and the path lengths traversed too short for these events to interfere with signals. For this reason, with respect to transmission media, we are generally more concerned with permanent, cumulative degradation resulting from TID.

Ionizing radiation causes charge to become trapped by defects in the optical medium, creating color centers. Once the color centers form, light transmission efficiency is degraded as the color centers absorb signal photons. The degradation, however, need not be permanent. As is the case for trapped charge in microelectronics, color centers can heal by annealing. The processes of formation and annealing of color centers take place in competition, and optical medium degradation depends on the relative rates of these mechanisms.

Light absorption in the medium will result in a decrease in the Photodetector Output Current for current transfer applications. For data transfer applications, the device ability to transmit data will be compromised. We note that for most, if not all, optocouplers the signal path lengths through the coupling medium are relatively short (<0.5 cm), these loses due to TID are likely negligible for most optocouplers.

III.C.3 Permanent Damage in Optical Detectors

The purpose of the detector in an optocoupler is to detect optical signal and convert it into an electrical current. Here we consider the effects of TID and DDD on the most common optical detectors [Barn-84, Wicz-86, Mars-92].

Optical detectors in optoelectronic devices function by detecting the photocurrent generated by a photon with energy greater than the semiconductor bandgap. For this reason, any damage to the semiconductor that changes its global properties, or that degrades the semiconductor's ability to carry a current will potentially compromise the detector's efficiency.

As TID accumulates, photodetectors degrade, with leakage currents increasing up to several orders of magnitude for doses up to 1 Mrad(Si). Both TID and DDD increase background noise, and DDD tends to decrease current outputs. However, many photodetectors show remarkable robustness to surviving space radiation environments.

IV. Assessment of Single Event Transient Sensitivity

IV.A Introduction

Data at the output of an optocoupler can be corrupted by ionizing radiation if the following conditions are met simultaneously:

1. The charge collected by the photodetector is above some critical charge for inducing the effect.
2. The emitter illuminates the photodetector in such a way that the charge generated by the ion track is a significant fraction of the total liberated charge, i.e., sum of ion-induced and photon-induced charge. Typically, optocoupler drive currents are such that this condition occurs when the emitter is off.
3. The bandwidth of the optocoupler is sufficient to allow the transient to propagate.

Meeting the above criteria is necessary but not sufficient to induce data corruption. The data is only corrupted when the transient produced on the output of the optocoupler propagates through the follow on circuitry and the transient is detected as erroneous data. Prediction of the occurrence of a transient at the output does not constitute a loss of data. An analysis of the affect of the SET on the system must be carried out (see [SEECA]).

IV.B Test Guideline for Evaluating Optocoupler SETs

Below we present a test guideline that should be used when evaluating an optocoupler for space radiation induced SETs. This set of guidelines are intended to augment and supplement [F1192] and [p+ LL] and deals only with specific concerns for optocoupler transient testing. Radiation facility issues like particle beam counting methods, beam energy measurement, beam stability and uniformity, methods for testing in vacuum chambers will not be addressed.

Guideline IV.B.1: Radiation Species Selection for SET Testing

In high bandwidth optocouplers, both proton direct ionization and proton induced nuclear reactions can cause SETs. Therefore sensitivity should be investigated using protons.

Transients induced by heavy ions in the optocoupler's output amplifier can contribute to the total SET cross-section and can last longer [John-98]. Heavy ion testing should be carried out if the SEE environment is not dominated by protons, or if the coupler bandwidth is low.

Guideline IV.B.2: Recommendation on Characterization of Heavy Ion SET Over Particle LET

The classical approach for characterizing the SET cross-section over particle LET can be used to measure the sensitivity of an optocoupler to heavy ions (Z>1). See [F1192M, JEDEC HI] and the IEEE Nuclear and Space Radiation Effects Short courses for a detailed discussion on the classical approach for heavy ion SEE measurements.

Guideline IV.B.3: Recommendations on Proton Energy Selection and Angle of Incidence

Two different approaches for SET rate predictions have been suggested. (These rate prediction methods are summarized further in Section IV.C of this guideline.) Reed, et al., recommended a combination of the Bendel method for proton induced SET by nuclear reactions along with the traditional Integral Right Rectangular Parallelepiped (IRPP) method for direct ionization. Johnston, et al., recommended an empirical approach based on angular dependent SET cross-section data measured at multiple proton energies [John-99b], called the direct integration method. The choice of rate prediction method defines the type and amount of data required for the analysis. Any proton-induced transient rate prediction technique for optocouplers must include effects due to direct and indirect ionization.

Table IV.B.2 gives a minimum selection of the proton energy and angle for the two methods rate prediction methods. For the table and the discussion below 0 degrees is considered to be normal incidence to the photodetector and 90 degrees is grazing along the long axis of the photodetector.

The Bendel-IRPP requires using at least one proton energy over a range of angle of incidence. (This test approach is identical to the classical approach of using angle of incidence to change the effective LET for heavy ion testing.) The energy selection should between 40 to 200 MeV so that the typical packaging thickness and diode length does not degrade the proton energy as it traverses the package and die. (Packaging material may need to be removed, see Guideline IV.B.4) Finer grid of steps in angle of incidence than that giving in **Table IV.B.1** will be necessary if the cross-section increases significantly between 60 and 80 or 30 and 60. Also, depending on the results, the angle of incidence might need to be greater than 95 degrees if the cross-section data has not peaked and began to roll off at 95 degrees.

The direct integration method requires that the angular dependence be measured for an estimated minimum of four proton energies. The goal for testing at the higher energies is to determine the saturated revised cross section (see Section IV.C). The lower energy testing determines how this revised cross section increases with decreasing energy. Both ends of the revised cross section curve must be characterized.

Table IV.B.1
Comparison of proton energy and angle selection for the two methods

Method	Example Proton Energy Selection	Example Angle Selection (degrees)
Bendel-IRPP	Single energy between 40 and 200MeV	0,30,60, and 80 to 95 in 1 degree steps
Direct integration	15,30,63,200 MeV	0,30,60, and 80 to 95 in 1 degree steps

Guideline IV.B.4: Recommendations on Package and Coupling Medium Removal for Proton and Heavy Ion Testing

A careful analysis must be carried out to determine if the proton energy remains constant as it passes through the photodetector. This needs to be verified for all angles of incidence. In order to achieve grazing angle data the side of the package may need to be ground away, and the coupling medium and LED may need to be removed in order to allow the protons to traverse the photodetector with a nearly constant energy.

The existing heavy ion irradiation facilities do not currently have sufficient penetration depth to reach the sensitive circuits if the packaging, LED or coupling medium remain intact. Therefore, for heavy ion testing, (as with all other heavy ion testing), in the direction of the ion beam, there must be a direct line of site to the die containing the photodetector and the amplification circuitry (if it exist).

Guideline IV.B.5: Fluence and Flux Recommendations

As with all SEE testing, the flux must remain low enough not to cause pile-up of data collection. This can occur either because of bandwidth of the optocoupler or the efficiency with which the data is stored by the data collection system.

The minimum fluence that should be used is related to the acceptable statistics. Typically, 25 to 100 events of each type that can cause a system impact is acceptable. The SEECA [SEECA] process should be used to determine the types of events that are system critical.

Guideline IV.B.6: Method for Achieving Desired Proton Energy

There are two methods to achieve a specific proton energy.

1) Tuning the cyclotron to the desired energy. Most accurate method.
2) Using a degrader to reduce the energy. Much faster than tuning.

If a high degree of accuracy is desired then the tuning method will be the best choice.

The data in **Figure IV.B.1** shows that a 60 MeV proton beam degraded to 30 MeV gives different results than a proton beam tuned to 30 MeV. The degraded beam gives higher cross-sections and the increase in cross-section appears at lower angles. The increased width in the response around grazing incidence is due in part to the increase in beam divergence from multiple scattering interactions. **Figure IV.B.2** shows the results of TRIM calculations indicating the change in proton trajectories resulting from degradation from 60 MeV to 30 MeV average energy. In that case, again the scattering and energy straggling in the degrader material produces a distribution of protons with lower energies, and consequently, higher LETs.

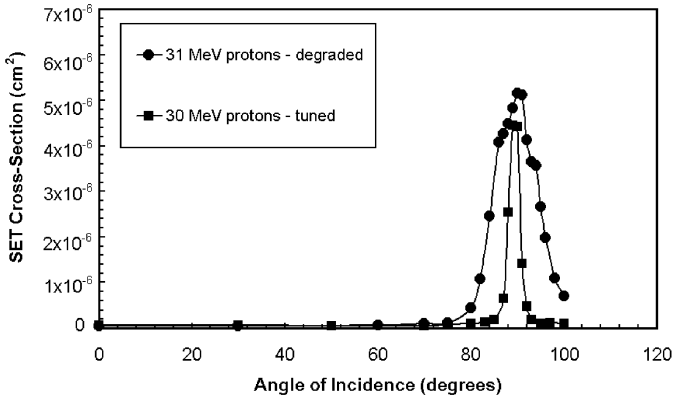

Figure IV.B.1
Comparison of SET cross-section measurement for degraded and tuned 30 MeV proton beam on the Agilent HCPL5231 optocoupler [Reed-01].

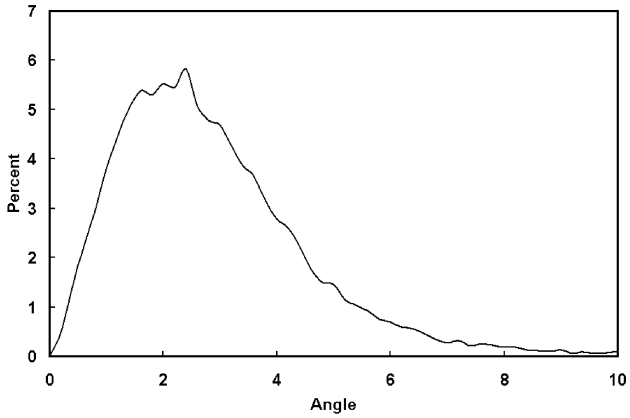

Figure IV.B.2
TRIM calculation for trajectory of a 63 MeV proton after passing through 1.2 cm of Al.
The exiting energy was ~ 30 MeV.

Guideline IV.B.7: Recommendations on SET Data Collection Techniques

The test circuit depicted in **Figure IV.B.3** replicates a typical circuit implementation of the optocoupler for a satellite application. Using this circuit can be used to examine the possibility of transients in both the illuminated and in the unilluminated states [Reed-98]. This discussion is useful for heavy ion and proton testing.

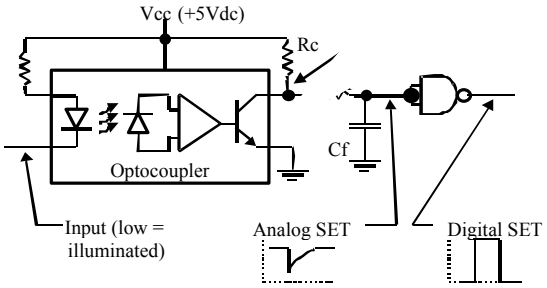

Figure IV.B.3
Schematic representation of transient test circuit showing the filter network and the two probe locations for analog and digital transient capture.

Measurements are conducted using an embedded National Instruments™ controller running Labview™ software. The core of the test was a 5 Gsps (Giga samples per second) digital oscilloscope manufactured by Tektronix™ (model TVS625) and its companion 1.5 GHz bandwidth active probe (model P6245). Additional equipment consisted of a digital I/O for controlling and monitoring the test board, GPIB power supply for the support circuitry as well as the DUT, and current monitoring.

Care must be given to the type of oscilloscope probe that should be used at different points in the circuit. A DC signal from the experiment controller is buffered and fed to the optocoupler. The optocoupler open-collector output is sampled by an oscilloscope with a high-speed, low capacitance active FET probe. It also feeds either an AC or ACT logic gate buffer. The transient monitored at the optocoupler output will exhibit the analog characteristics of the SET, but the buffered signal will generally be a clean TTL or 5V CMOS level signal. The buffered signal is sampled by a passive oscilloscope probe. The buffered signal is fed to a conditional inverter along with the DC signal controlling the optocoupler input. Thus, the output of the

conditional inverter is always nominally logic level LOW, with a SET always appearing here as a positive-going pulse. **Figure IV.B.4** shows an example of a transient SET captured at the probe points indicated in **Figure IV.B.3**.

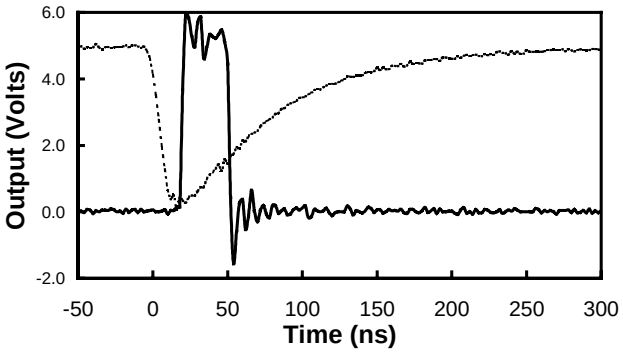

Figure IV.B.4
A typical transient from the HP6631 optocoupler as measured at the optocoupler output and at the circuit output as indicated in the previous figure. The filter values were: Rc = 2.0 Kohm, Rf = 0 ohm and Cf = 0 pf.

Guideline IV.B.8: Circuit Level Application Specific Testing Must be Performed

The transient response is very dependent on the application. It is critical that all circuit configurations be tested. The circuit parameters can be varied for the test configuration given in **Figure IV.B.3**. The optocoupler output stage is open-collector, and the value of the collector resistor, Rc, affects the response of the circuit to SETs. The circuit response is additionally affected by capacitance on the node. Both of these values were made changeable and were test variables, as was the supply voltage to the optocoupler and the RC filter added to the circuitry to investigate mitigation techniques.

Table IV.B.2 illustrates the circuit response to varying resistor combinations in the passive filter circuit. The event cross sections and event durations at the output of the analog circuit reflect the ability of the filter to shorten the transient duration and reduce the total number of events reaching the circuit output. In all cases, the value of Cf was 0 pf. For the cases shown, the more dramatic effect corresponds to the addition of a series resistance (Rf). The resulting RC network tends to suppress the transient propagation to the output, but it also compromises the circuit bandwidth, which in some applications may be unacceptable.

Table IV.B.2
Passive filtering of transient events impacts measured cross-section and duration.

R_c Ω	R_f Ω	< 20 ns	20 – 40 ns	40 -60 ns	Total Events	Cross Section (cm^2)
5.11K	0	2	7	32	41	4.3E-08
2K	0	4	29	6	39	4.1E-08
511	0	7	23	2	32	3.4E-08
2K	2K	18	1	0	19	2.0E-08
511	2K	12	0	0	12	1.3E-08
511	5.11K	0	0	0	0	1.0E-10

Guideline IV.B.9: Characterize SET Pulse Width and Amplitude as a Function of LET

The pulse width and amplitude of the SETs is a function of particle LET. **Figure IV.B.5** shows histograms of pulse widths for various particle LETs for the HP 6N134 [John-98]. Characterization of this type must be done over particle LET so that system impact can be assessed.

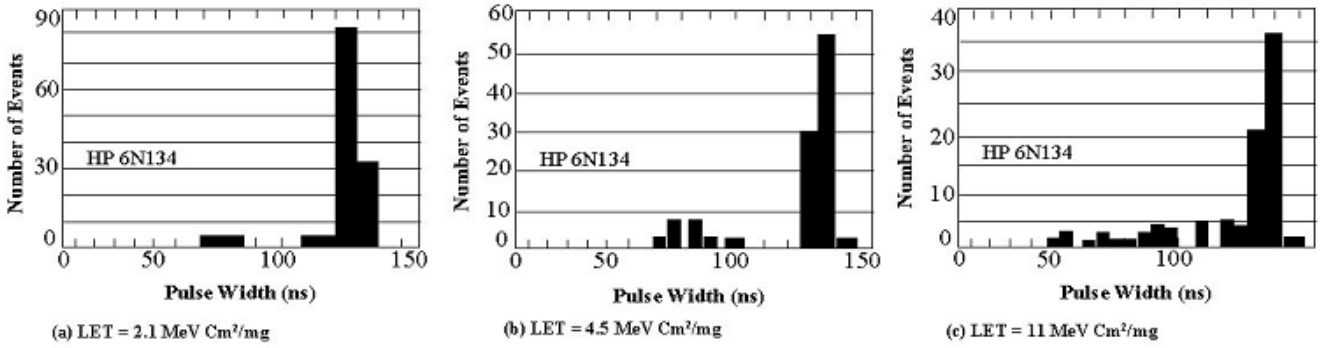

Figure IV.B.5
Pulse width distribution for HP 6N134 for various LETs.

Guideline IV.B.10: DUT Sample Size

Test data collected has shown significant part-to-part variability in optocoupler SET susceptibility. In **Figure IV.B.6**, we can see a ratio greater than 2 between the maximum cross-section for the two tested parts. (A 31 MeV proton beam energy was achieved by degrading a 63 MeV beam.) It is recommended that the test be performed on a sufficient number of parts coming from the flight lot to characterize this variability.

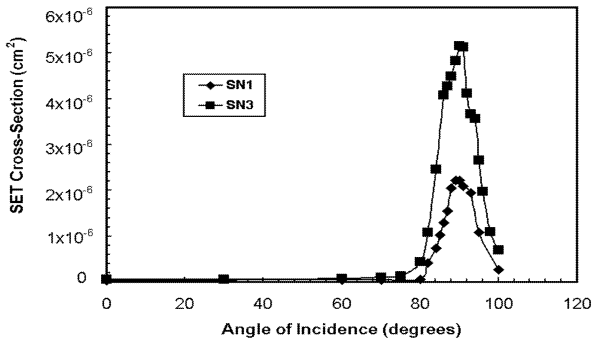

Figure IV.B.6
Example of part-to-part dispersion observed during proton SET characterization of the Agilent HCPL5231.

IV.C Summary of Rate Prediction Approaches

Two approaches to SET rate predictions have been reported. Reed, et al., recommended a combination of the Bendel method for proton induced SET by nuclear reactions along with the traditional Integral Right Rectangular Parallelepiped (IRPP) method for direct ionization. It calls for using a LET distribution describing the combined proton and heavy ion environments, also the a cross-section versus LET curve includes the combined proton and heavy ion characterization results [Reed-98]. Johnston, et al., recommended an empirical approach based on angular dependent SET cross-section data measured at multiple proton energies [John-99b], called the direct integration method. Both methods give similar results as shown in **Table IV.C.1**. The

advantage of the Bendel-IRPP method is that it uses the traditional tools for SEE rate prediction and it requires less experimental data.

The rate prediction methods for fiber optic data links and optocouplers is described in [MG]. Carefully following the methods described in [MG] is essential when estimating the SET rate for optocouplers. The text that follows contains a summary of [MG], the reader is strongly encouraged to review [MG].

Table IV.C.1
Comparison Of The Transient Rates Obtained With The 2 Methods On The Agilent 6N134 Optocoupler For A 705km , 98° Circular Orbit Behind 100 Mils Of Al Shielding, 50 mm Thickness. [Reed-01].

	Total number of transient/year	**Number of Transients/year induced By indirect ionization**
Direct Integration Method	1,665	470
Bendel-IRPP Method Results	1,200	400

IV.C.1 Example of Bendel-IRPP Rate Predictions Method

In this section we present an example of an optocoupler that has experienced SETs in the space environment to demonstrate the use of the combined Bendel-IRPP rate prediction methods.

The Motor Drive Amplifier (MDA) of the High Gain Antenna (HGA) on the Terra satellite has experienced several anomalies (shutdown of the MDA) since the launch in December 1999. Analyses have shown that this anomaly is due to SETs in the Agilent HCPL-5231 optocouplers. Detailed studies of the flight hardware configuration showed that an SET induced pulse lasting at least 100 ns on the output of the optocoupler could trigger this event.

There were 135 anomalies observed between December 20, 1999 and January 26, 2001. **Figure IV.C.1** shows the location of the anomalies. Of these, 105 anomalies occurred in the South Atlantic Anomaly (SAA) proton region. Among the 30 events that did not occur within the SAA, 23 occurred during the July 14th and November 9th Solar Particle Events. The other 7 events occurred in the high latitude regions of the orbit and are attributed to GCRs.

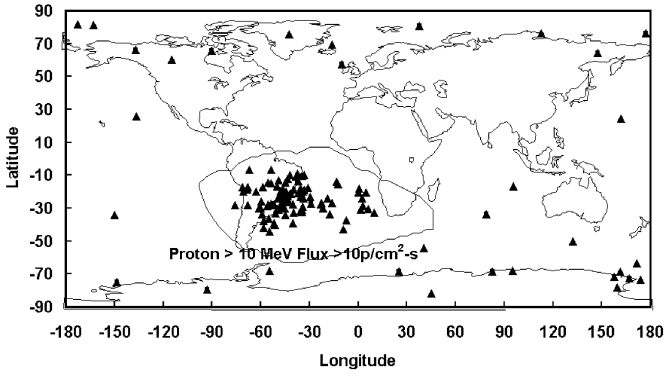

Figure IV.C.1
Location of the Terra HGA events. These events have been shown to be a result of SETs induced in an Agilent HCPL5231 [Reed-01].

SET testing was performed at University of California at Davis (UCD) with protons and at Brookhaven National Laboratory (BNL) with heavy ions. During testing, the bias conditions were identical to the application conditions. **Figure III.B.3** presents some of the proton SET cross-section versus angle of incidence data. The data in **Figure IV.C.2** present the measured SET cross-section versus effective LET for heavy ions and protons. The proton cross-section points are obtained by applying a cos(θ) correction to the fluence used in the cross-section calculation. Then we assign an effective LET, defined as the product of the particle's LET and sec(θ). Note that the proton data and the low LET heavy ion data are consistent. The LET dependence of both the heavy ion and proton cross-section data were then approximated by a Weibull distribution. The proton data at 0 degrees incidence are used to build the proton cross-section curve versus energy. This curve is then fitted with the Bendel model.

The CREME96 software was then used to define the environment (GCR and trapped protons integral LET spectra and GCR protons and trapped protons energy spectra). The CREME96 HUP routine was used to calculate error contribution for direct ionization events, and the PUP routine was used to calculate the error rate for indirect ionization proton events. A discussion of the warnings and concerns when using CREME96 HUP for this type of calculation is given in [MG].

Optocoupler's detectors uses a conventional bipolar processing method, thus diffusion from the substrate bulk may be significant. Characteristics of optocoupler cross-section measurement consistent with charge collection via diffusion were first noted in [LaBe-97], and later investigations [John-99b, John-98] indicated that diffusions lengths approached 50 μm. For these thick aspect ratios, the ability of the RPP geometry to represent the actual circular cylindrical detector geometry could be a concern. [MG] discusses this issue and others concerning rate prediction tools.

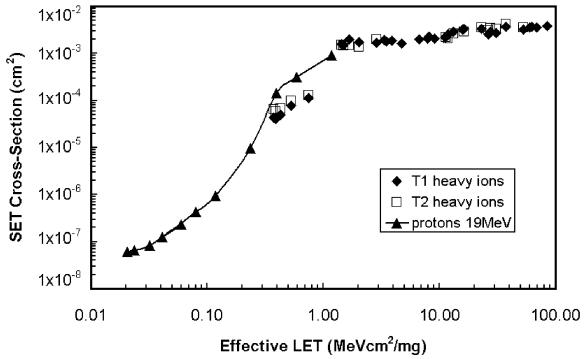

Figure IV.C.2
Transient cross-section for heavy ion and proton effective LET [Reed-01].

The rate calculation was made assuming the solar maximum radiation environment for the Terra orbit (circular 690 km, 98° inclination orbit) and including the effects of 300 mils Al shielding. We also assumed a 50 mm sensitive volume depth to estimate the SET rates with PUP and HUP routines of CREME96. The estimated upset rate induced by Galactic Cosmic Rays (GCR) is 0.05/day and the upset rate induced by trapped protons is 1/day. Proton direct ionization accounted for about 70% of this rate. The total upset rate for the MDA is three times the upset rate of one optocoupler when the MDA motors are moving. These motors are moving about 40% of the time. So the estimated upset rate for the MDA is about 1.2/day. Since the observed rate is about one event every 3.3 days, this predicts the on orbit rate to within a factor of 4.

Based on the uncertainties in the prediction method (size of the sensitive volume, AP8 model uncertainties, absence of detailed shielding analyses, etc.) and the very significant part-to-part variation, we consider that the prediction is in very good agreement with the on orbit event rate. The estimated upset rate for Galactic Cosmic Rays (GCR) was ~0.05/day, which is in good agreement with on orbit data (~20 predicted versus 7 observed).

IV.C.2 Rate Prediction Method by Direct Integration

In [John-99b] an empirical approach was suggested for photodetectors used in optocouplers. This approach requires data to be collected at several angles of incidence and at several proton energies. One then integrates these data over the proper on-orbit proton spectra. The first step is to integrate the cross-section over all angles at each energy. Angular data like that in **Figure III.B.3** must be collected at all energies and then integrated over all angles to arrive at an effective cross-section curve like that in **Figure III.D.1**. The next step is to integrate this effective cross-section with the space proton environment.

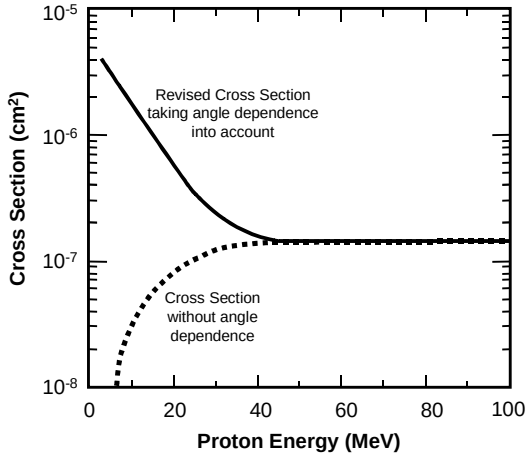

Figure III.D.1
Effective cross-section—including the angular distribution like that in Figure IV.A.2—for various proton energies on the HP6N134 [John-99b].

V. Assessment of Permanent Degradation

V.A Introduction

TID and DDD can severely degrade the performance of an optocoupler. The most studied effect is how radiation degrades Current Transfer Ratio. CTR is defined as the ratio of the output current (I_C) to the input current (I_F) (See **Figure V.A.1**). The concepts described here can be used to assess the degradation of any circuit parameter that depends on optocoupler CTR.

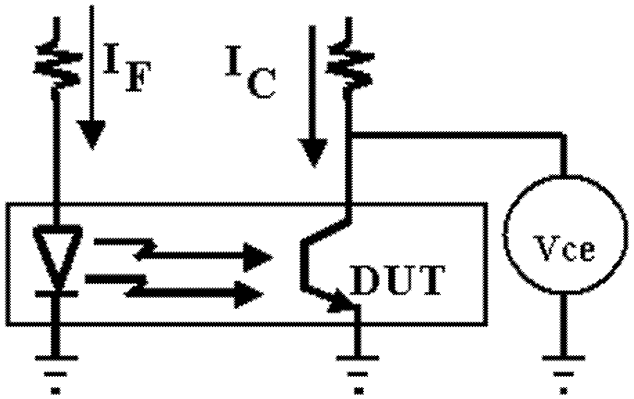

Figure V.A.1
Schematic showing experimental setup for measure CTR degradation.

A full characterization of all optocoupler parametrics like switching speed, leakage current, etc… are required to assess the performance of the device in the space radiation environment. For TID induced effects, this assessment should follow the guidelines in ASTM Standard 883: Test Method 1019.5. Also, the concepts for assessing DDD described below for CTR can easily be adapted to other parametrics.

Assessing radiation degradation of CTR is complicated by several factors:

- observed radiation induced degradation results from a combination of ionizing dose and displacement damage mechanisms, each affecting the individual optocoupler components differently [Rax-96, Reed-98].
- lack of consistency between experimental determination of damage factors for LEDs and theoretical calculations for NonIonizing Energy Loss (NIEL) in III-V materials precludes use of NIEL to describe the energy dependence of displacement damage effects [Mars-99, Reed-00]
- application specific testing is necessary [D'Ord-97]
- optocoupler radiation response exhibits large part-to-part variability [Reed-01].
- injection current can anneal the displacement damage-induced degradation of LED light output [Barn-84, John-99a]
- temperature and lifetime effects impact CTR [Reed-01]

Some of these concerns need to be addressed when estimating exposure levels, others during the testing phase of the risk assessment, and others must be considered in combination with radiation-induced degradation estimates to give overall performance. Each of these complications will be addressed in more detail during the discussion of the risk assessment approach.

V.B Risk Assessment Approach

V.B.1 Introduction

TID and DDD can degrade the CTR of many optocouplers, as demonstrated in **Figure V.B.1** which compares degradation for gamma ray exposures of a Texas Instruments (TI) 4N49 to that for 195 MeV proton exposures. Proton irradiations cause significantly larger degradation than gamma ray exposures at equivalent doses. This type of optocoupler response is due to the greater amount of displacement damage for proton over gamma exposures [Rax-96]. A comprehensive radiation risk assessment must include both degradation mechanisms. This section will discuss each block of the radiation risk assessment approach; the concerns listed above will be address when applicable.

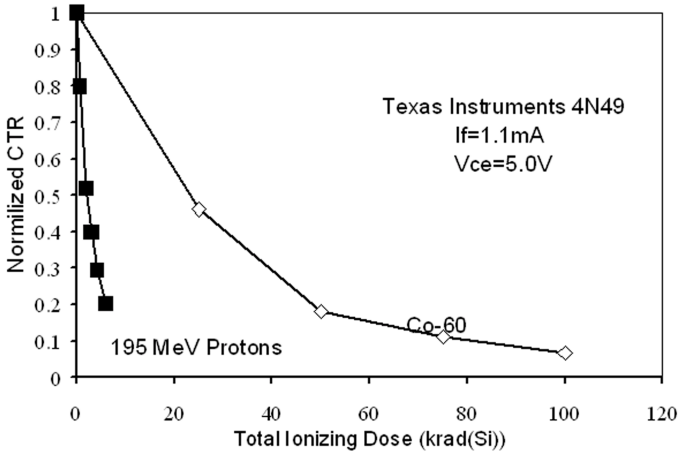

Figure V.B.1
Gamma and 195 MeV proton irradiations of Texas Instruments 4N49 [Reed-98].

Figure V.B.2 shows our current approach for assessing the impact of the space radiation environment on optocoupler CTR. In this method, separate tests are conducted for both mechanisms. Then the results are combined to estimate the CTR degradation for a specific mission DDD and TID.

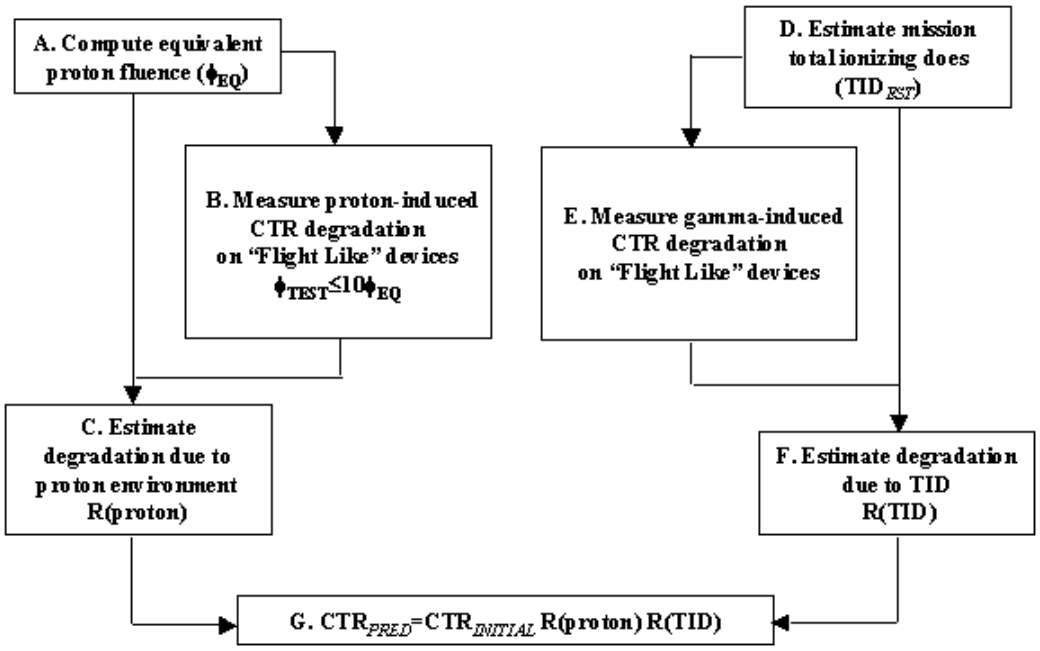

Figure V.B.2
Process for estimating CTR degradation [Reed-01].

V.B.2 Step-A: Compute Equivalent Proton Fluence

It is beyond the scope of this guideline to describe in detail how to compute the differential proton fluence for a mission. We refer the reader to [Bart-97] for a discussion on performing this calculation. This estimate should include any radiation design margins.

The worst-case mission "equivalent" fluence (ϕeq) is estimated by a "manufactured" worst-case damage function. This function is constructed piecewise from segments of either the calculated NIEL curve for the specific III-V material [Mars-99] or the curve from experimental displacement damage measurements on the LEDs in question [Barr-95, Reed-00]. The "manufactured" worst-case curve is the combination of these curves that results in the worst-case equivalent fluence for the test energy in question. The contributions to ϕeq from above and below the test energy are determined separately and added together to get ϕeq. The ϕeq must be computed for each test energy.

The need to determine ϕeq is driven by the lack of consistency between theoretical calculations for NonIonizing Energy Loss (NIEL) in III-V materials and experimental determination of damage factors for LEDs.

V.B.3 Step-B: Guideline for Measuring Proton-Induced Degradation

Proton testing is primarily used to assess the DDD effects on optocoupler CTR. However, for certain space flight missions that are dominated by a proton environment, proton testing can deliver sufficient TID to estimate the both DDD and TID-induced degradation. This will be discussed further in the section on TID effects.

Guideline V.B.3.a: Test Fluence and Flux

The test fluence (ϕ_{TEST}) that should be used when performing ground testing to characterizing optocoupler CTR degradation should be greater than a factor of five over ϕ_{eq}. This is not a pass/fail fluence level; that is, it does not define the fluence level that should be used to simulate the expected on-orbit performance. Rather, it is a recommendation for the minimum value of the cumulative fluence used during the testing phase.

The effects are independent of proton flux. The flux should be controlled such that the fluence steps are within the dosimetry capabilities of the facility such that a +/- 10% uncertainty in total fluence is maintained.

Guideline V.B.3.b: Recommendation on Number of Irradiation Steps and Fluence at Each Step

CTR must be measured prior to irradiation and at several fluence levels up to ϕ_{TEST}. Making multiple measurements of CTR allows for characterization of the degradation to be fully mapped out over ϕ_{TEST} (for example see proton data in **Figure V.B.1**). These data provide the CTR degradation curves used to estimate CTR degradation in Step-C. If there is no current knowledge on how the device is going to perform we recommend starting at $1x10^8$ p/cm^2 for amphoterically dope LEDs and $1x10^9$ p/cm^2 for double heterojunction, then increasing the fluence steps linearly on a log scale, i.e. $1x10^8$ p/cm^2, $3x10^8$ p/cm^2, $5x10^8$ p/cm^2, $1x10^9$ p/cm^2, and so on, until ϕ_{TEST} has been reached. This can be done for one device so to guide the test for the complete sample size

***Guideline V.B.3.c: Proton Test Energies*:**

Multiple Proton Test Energy Option

Figure V.B.3 plots the normalized lifetime-damage factors (K) for single heterojunction LEDs to NIEL as calculated by Summers et al. [Burk-87, Summ-88] (solid curve) and the results obtained by Barry et al. on amphoterically doped [Barr-95] (open squares). Similar trends have been observed for double heterojunction LEDs [Reed-00]. For this plot, the NIEL values are normalized to the values at 10 MeV. It is clear that the current data sets agree better with the experimental data from [Barr-95] than with the NIEL calculation [Burk-87, Summ-88].

Because of the inconsistency between experimental determination of damage factors for LEDs and theoretical calculations for NIEL [Reed-00], we do not recommend using NIEL to determine the mission equivalent fluence for a single test energy. Instead, we recommend that a suite of energies be used. Proton test energy selection should be based on the expected space radiation environment (including shielding effects). An example of a suite of proton test energies for LEO mission with 100 mils shielding would be 200, 100, 60, 35 MeV, and lower if package penetration considerations allow knowledge of the energy reaching the internal components.

Single Proton Test Energy Option

Figure V.B.4 plots the various equivalent test fluence of 50 MeV or 200 MeV protons one would require to predict output power degradation due to damage from a combination of trapped and solar protons for a five year mission in a 600 km x 90 degree circular orbit. The equivalent fluence is given for NIEL and for the trend given by experimental data in **Figure V.B.3**. For lightly shielded applications, this figure shows a large difference in the estimated mission equivalent fluence depending on which energy dependence is assumed in the calculation. This discrepancy disappears for heavily shielded applications. This is because low energy protons are more easily stopped by shielding. For example, if the normalization were made at 200 MeV the NIEL correlation would lead to underestimation of the damage by a factor of 7 for a device with 50 mils Al shielding. This magnitude of error could be disastrous. Normalization to test data at 50 MeV with the NIEL correlation shows a factor of 3 underestimation which is less dramatic, but significant nonetheless.

It is possible to use a single energy to estimate a conservative estimate for the on-orbit CTR degradation if the project were willing to carry a medium risk level. The only way to insure low risk is to collect energy dependence data. The test energy should be selected such that it is near the low energy side of the peak in the differential proton spectra, we recommend that this energy not exceed 63 MeV. (The proton energy must be sufficient to penetrate the packaging and have a known and constant energy throughout the optocoupler active components.) Using a single test energy imposes high margin requirements for medium risk (Step-D).

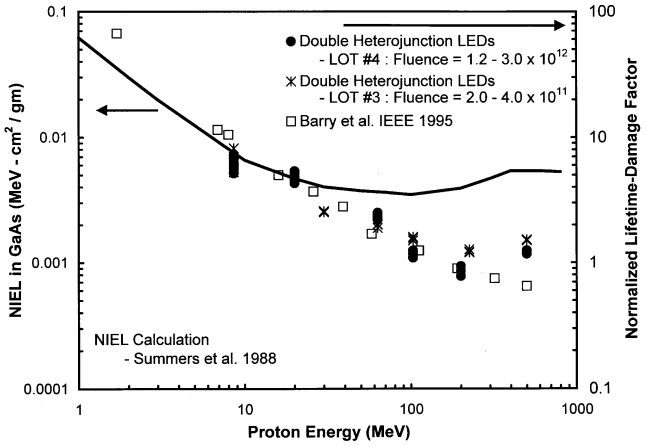

Figure V.B.3
Lifetime-damage-factor measurements for double-heterojunction devices (scaled to the right abscissa), normalized to agree with calculated NIEL values (solid line—scaled to the left abscissa) for 10 MeV protons [Reed-00].

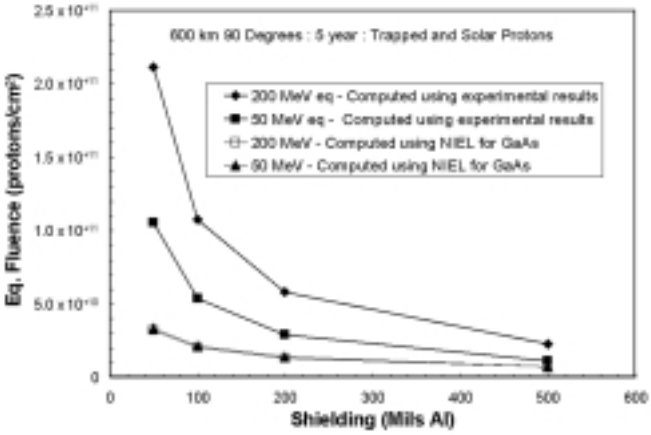

Figure IV.B.4
On-orbit degradation for a mission (in this case 5 years, altitude 600 km, inclination 90) can be predicted with a given fluence of protons, regardless of energy—provided displacement damage is proportional to NIEL. If damage follows experimental trends of Barry et al. proton beams of different energies require different equivalent proton fluences to inflict the same damage—especially for lightly shielded applications [Reed-00].

Guideline V.B.3.d: Recommendation on Test SET Configuration

Device characterization must consider application specifics. **Figure V.A.1** shows the experimental setup used to replicate several different application. Gummel plots for collector current (I_C) are taken for various forward current (I_F) and V_{CE}. We recommend using a parametric analyzer to measure these Gummel plots. The

resister on the collector side of the photodetector can be a variable resistive load (R_L) that is used to simulate different applications.

For this setup, sweeping the voltage (V_O) supplied to photodetector and R_L series causes V_{CE} to change for fixed I_F. The collector-emitter voltage (V_{CE}) is the difference between V_O and the voltage drop across R_L.

The pre-irradiation Gummel sweeps of a Texas Instruments 4N49 optocoupler are shown in **Figure V.B.8**. The I_C is plotted as a function of the I_F for various V_{CE}. Notice that I_C increases proportionally with I_F with a slope governed by the current gain (analogous to the active region for simple transistors). When the optocoupler is fully on, this proportionality breaks down, and the curves for various V_{CE} values flatten out at nearly constant values of I_C. Further increases in I_F result in very small increases in I_C (analogous to the saturation region for simple transistors).

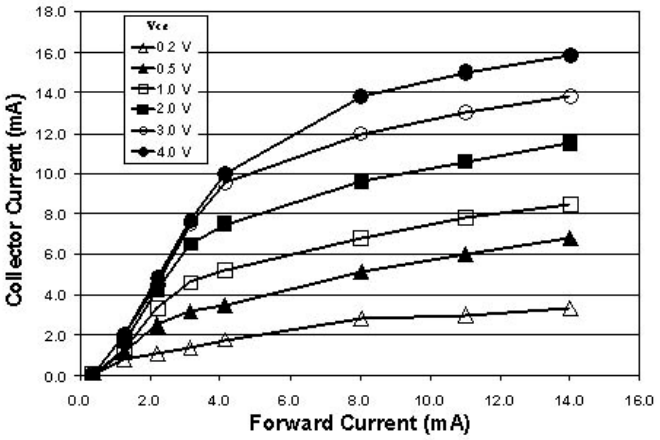

Figure V.B.8
Pre-irradiation I-V characteristics of a TI 4N49. Radiation damage changes the shapes of these curves [Reed-98].

As was described in the previous section, displacement damage can degrade each component of an optocoupler. The impact of this degradation is seen in how the shapes of the curves shown in **Figure V.B.8** change with radiation damage. These shapes of the curves can change when the optocoupler is exposed to either an environment that induces DDD or deposits TID. Gummel plots can be used for TID measurement of CTR degradation.

An important point here is that if V_{CE} is held at a constant value during testing, then the response of the device to radiation will be different than the case where V_{CE} is changing due to radiation-induced effects.

Consider the following two applications involving two forward currents: I_F = 8mA (analogous to saturation region for simple transistor) and I_F = 1mA (analogous to active region of simple transistor). Further assume that the major degradation mechanism is LED light output degradation (believed to be the dominate mechanism for this type of optocoupler). Light output degradation of the LED is analogous to a reduced base current in a simple transistor. Reduced light output due to radiation can also be viewed as having the same effect as reducing the forward current in an unirradiated device, i.e. degraded light output due to radiation or reduced drive current will both reduce I_C. If the forward current is changed while the device is in saturation, the collector current, and hence the CTR, will remain essentially constant. However, if the forward current is changed when operating in the active region then the optocoupler I_C will change. It is easy to see from this that different values for V_{CE} will give different radiation responses.

The data represented by solid filled symbols connected by solid lines in **Figure V.B.9** show a comparison of the CTR degradation at two different loads (R_L) for the same device (V_{CE}=0.3V for both loads). The test conditions that existed during the 2.7 ohm measurements are consistent with holding V_{CE} constant at 0.3V. We note that the CTR for the case where the load was 2.7 ohm degraded by almost 50% of its original value after an

exposure of $1x10^{11}$ p/cm^2 while the 1 kohm load degradation was 92% of the original value. This is nearly a factor of two difference for the same initial conditions.

The dashed lines in the figure show the radiation-induced change of V_{CE} with fluence for each load. For the 2.7 ohm load case V_{CE} is remained constant at 0.3V. In the case where the load is 1 kohm, V_{CE} increased with increasing fluence. Radiation degraded the output of the LED, as evident in the 2.7 ohm loading, but for the 1 kohm loaded case output degradations was compensated for by an increase the emitter-collector voltage. These data clearly show that a significantly inaccurate prediction of CTR degradation would occur if application specific testing was not carefully done for this type of application.

The data represented by the unfilled squares in **Figure V.B.9** show the CTR degradation for a fixed Vce of 5 V. The last data point on this curve shows a degradation of 29% of the original value. Compare this to the 92% when V_{CE} was allowed to change (1 kohm load). Data collected at V_{CE}=5V over predicts the degradation in the 1 kohm load case by a factor of 4.6, a significant impact on performance predictions when application specifics are not considered.

These data are clear evidence that, in order to accurately characterize the radiation degradation of CTR for optocoupler operating in the saturation region, one should test the devices using the exact application parameters. Several publicly accessible databases and journals give data collected at fixed V_{CE}. If these data are used for certain applications then they could significantly over predict the degradation.

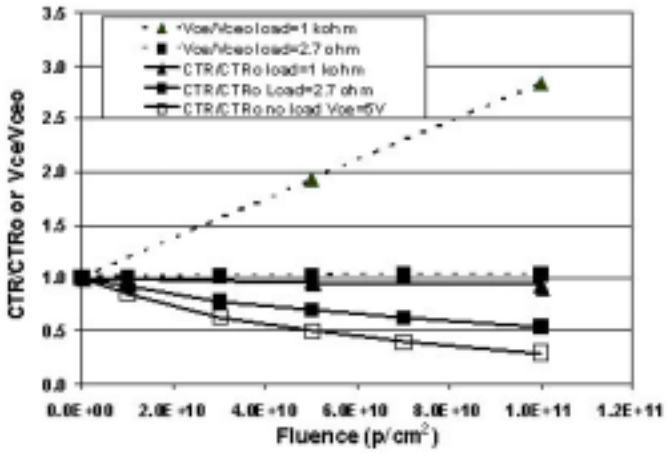

Figure V.B.9
Plot of either normalized CTR (solid lines) or normalized Vce (dashed lines) for a 4mA forward current. This shows the load dependence on the radiation response. It also demonstrates that testing at a fixed Vce would significantly over predict the CTR degradation [Reed-98].

Guideline V.B.3.e: Sample Size

The sample size must be large enough to characterize part-to-part and lot-to-lot (same lot can not be guaranteed) variations. There is no current guideline for the exact number that is required when testing COTS devices.

Since optocouplers are typically COTS hybrids, it is not surprising that they often exhibit large part-to-part variability. Some of this variation is due to the complication of having several different components that can be sensitive to various effects. **Figure V.B.3** shows data collected on three Mitel 3C91C optocouplers. At certain fluences there is over a factor of two variations in the response to radiation. This optocoupler is manufactured as a radiation-hardened product, and the internal components were all selected from the same device lot. These hybrids do not contain a light pipe to guide the light between the LED and the detector, so the variation is due to the differences in the response at the component level.

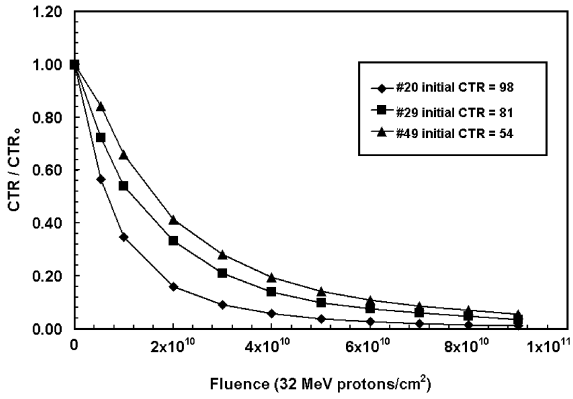

Figure V.B.3
Demonstration of part-to-part variability of CTR degradation within a single lot [Reed-01].

Another reason for part-to-part variations (and the most difficult to characterize) is the flexibility the vendor has in selecting the components internal to the optocoupler. **Figure V.B.4** gives data on Mirocpac 4N49. These data show as much as an order of magnitude variation in the sensitivity of these optocouplers from different "lots". As with all COTS devices, knowledge of the manufacturing process is very limited. Our recommendation is to acquire optocouplers from vendors with a history of providing devices that have consistent degradation characteristics, to test the devices from the "flight like" lot in a "flight like" configuration, and realize that there is still some unquantified inherent risk. This risk is inherent in the choice to use COTS on a space flight mission—a risk that must be accepted at the beginning of the mission design.

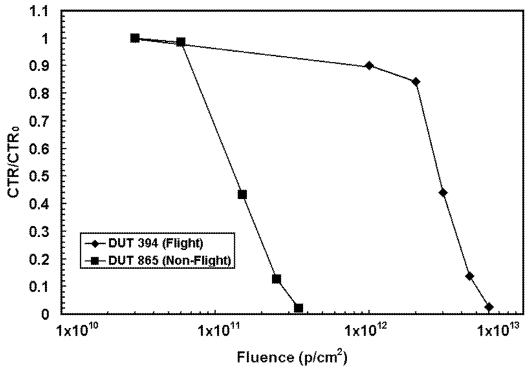

Figure V.B.4
Demonstration of lot-to-lot variability of CTR degradation [Reed-01].

Guideline V.B.3.f: Annealing of Damage

Injection current annealing of displacement damage-induced degradation of LED light output has been observed [Barn-84, John-98]. This has also been observed in optocouplers [Reed-01]. **Figure V.B.5** shows the recovery of the collector current under two annealing currents (1 mA and 10 mA) for three measurement forward currents (1, 5, and 10 mA). The data connected with the solid lines was annealed at 10 mA (unfilled symbols), while the data represented by the filled symbols where taken at 1 mA annealing forward current. The collector current is normalized to the pre-irradiation values. The ordinate is the amount of charge in coulombs that has passed through the LED during the annealing period. (So for 10 mA anneal, the time to reach 1800 coulombs is 50 hours, while the time to reach this charge for a 1 mA is 20.8 days.) The recovery factor shown

in the legend gives the ratio of the collector current after 1800 coulombs anneal to post-irradiation (prior to the anneal step) values for the collector current.

First note that for the annealing conditions between 100 and 1800 coulombs there is a correlation of the recovery between the 1 and 10 mA annealing conditions for all three test conditions. This implies that an accelerated annealing test could be used for these annealing periods, reducing the time to determine the amount of recovery by a factor of 10. If this accelerated annealing approach could be generalized then one could use it to estimate the annealing occurring over long mission times. However, in order to generalize this accelerated annealing test, more data on other part types is needed. Also, for missions with long annealing times, studies out to greater integral charge values will be required. This accelerated annealing approach should be studied in more detail before being implemented in a risk assessment approach.

The second interesting point that this data shows is the collector-current recovery-factor (the ratio of the annealed collector current to the post-irradiation value) is dependent on the forward current and the annealing current. The recovery factor is also dependent on the anneal time. All of these are application dependent issues.

Annealing should be minimized while collecting CTR degradation data over the test fluence. This can be best achieved if the optocoupler "on-time" (when the LED is illuminating the photodetector) is minimized and the forward current is minimized. Post-irradiation annealing studies at the anticipated forward current conditions and the "on-time" for the on-orbit application can be used to understand the margin in the final estimate of the on-orbit degradation (Step-G).

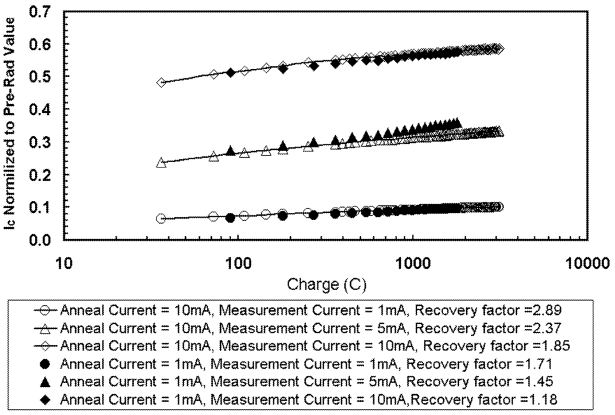

Figure V.B.5
Injection current annealing effect on collector current at two forward currents for three application currents. The data is normalized to the pre-irradiation collector currents [Reed-01].

V.B.4 Step-C: Estimation of Proton-Induced Degradation

Multiple Proton Test Energy Option

Testing over a range of energies allows the degradation to be estimated using a piecewise approach. The method bins the predicted (including any design margin requirements) space radiation particle fluence by test energy, and then uses the experimental CTR degradation curves (like those in Figs. V.B.1, V.B.3, and V.B.4) to determine the total degradation. For example, using the test energy suite for a given environment, one would sum up all particles with energies between 100 and 200 MeV and use the higher of the two measured CTR degradation rates over this energy range to estimate the degradation for this energy range. One would repeat this procedure for all energy ranges. The net degradation would be the sum over all energy bins.

For protons with energies too low to penetrate the package during ground testing, one must use the energy dependence of the calculated NIEL to estimate the damage rate. We strongly recommend that this only be used for energies less than 30 MeV, a region where the functional dependence of the calculations for NIEL nearly agrees with that for experimental data obtained on LEDs [Barr-95, Reed-00].

The sum of the estimated damage computed for each energy bin plus any additional degradation from lower energy protons gives an estimate of proton-induced on-orbit CTR degradation. R(proton) is defined as the ratio of the proton-induced degraded CTR to the initial CTR.

Single Proton Test Energy Option

When a single test energy is used the proton- induced degraded CTR can be determined using ϕ_{eq}. There is two cases that should be considered:

1. If, after the over test of ten times ϕ_{eq}, the CTR has changed by less than 5% then the proton-induced degraded CTR is the degraded CTR value at ten times ϕ_{eq}.
2. If, after the over test of ten times ϕ_{eq}, the CTR has changed by greater than or equal to 5% then the proton- induced degraded CTR is the degraded CTR at ϕ_{eq}.

In this analysis the energy dependence is assumed to follow the "manufactured" worst-case damage function described above.

V.B.5 Step-D: Estimate Mission Total Ionizing Dose

It is beyond the scope of this paper to describe in detail the methods used to compute the estimated mission TID (TID_{TEST}). We refer the reader to [Bart-97] for a discussion on performing this calculation. This estimate should include any radiation design margins for environment variability.

V.B.6 Step-E: Measure Gamma-Induced CTR Degradation

The discussion given in Step-B recommended using protons as the test environment for DDD effects. As discussed above, protons can also contribute significantly TID-induced degradation. If the mission TID level can be achieved during proton DDD testing, then the DDD and TID induced degradation of CTR is sufficiently measured during the proton testing, and TID testing using another ionizing dose source need not be carried out. However, if the TID delivered by the proton testing in Step-B is less than that delivered by the on-orbit ionizing dose sources then both proton testing (for DDD effects) and gamma (or any other ionizing dose source that has very limited DDD effects) testing must be carried out. The discussion that follows addresses "gamma-style" TID testing.

Typically, gamma or x-ray testing is used to simulate the space radiation TID environment. The dose level for TID testing (TID_{TEST}) should follow the guidelines in ASTM Standard 883: Test Method 1019.5. TID testing should include attention to application specific details (see discussion in Step-B).

CTR must be measured prior to irradiation and at several TID steps up to TID_{TEST}, for example see Co-60 data in **Figure V.B.1**. These data provide the CTR degradation curves used to estimate CTR degradation in Step-F.

V.B.7 Step-F: Estimation of TID-Induced Degradation

The degraded CTR is determined by the estimated mission TID (Step-D) and the measured CTR degradation (Step-E). The estimates should follow the guidelines in ASTM Standard 883: Test Method 1019.5. R(TID) is defined as the ratio of the degraded CTR value to the initial CTR.

V.B.8 Step-G: Estimation of Degradation

Multiplying the TID and proton-induced degradations gives an estimate for the on-orbit CTR degradation (CTR_{PRED}).

$$CTR_{PRED} = CTR_{INITIAL} R(TID) R(proton) \qquad (1)$$

Where $CTR_{INITIAL}$ is the initial CTR. This will allow one to determine the CTR margin that exists in a specific application. The margin is the ratio of the minimum CTR required to keep the application functional to CTR_{PRED}.

V.B.9 Interpretation of the CTR margin

Multiple Proton Test Energy Option:

The CTR margin defines the risk level that must be assumed. A margin between 0 and 2 is considered a high risk, a margin between 2 and 4 is a medium risk, and a margin greater than 4 is consider low risk.

Single Proton Test Energy Option:

If, after the over test of ten times ϕ_{eq}, the CTR has changed by less than 5% and the CTR margin is greater than ten this is consider a medium risk. If the CTR margin is less than ten the risk is high. Multiple energy testing can be carried out to reduce the risk.

If, after the over test of ten times ϕ_{eq}, the CTR has changed by greater than or equal to 5% the CTR margin is less than fifty then the risk is consider high, energy dependence data would be required to reduce the risk. If it is greater than fifty then the risk is consider medium.

The CTR margins of ten and fifty are empirical numbers that were derived by reviewing several data sets on various optocouplers.

V.C Recommendations

The approach defined above will yield a conservative estimate for CTR degradation. This is in part due to the exclusion of any annealing that may occur, in part that protons can induce damage via TID and displacement damage, and finally in part to the use of a worst-case "equivalent" fluence estimate. Although the above approach can be modified to account for these effect (albeit with reduced margins), we prefer to retain a conservative estimate—especially given the uncertainties associated with the use of COTS hybrid devices.

Temperature effects must also be considered when using the margins derived above to assess the likelihood of optocoupler survival when exposed to the space radiation environment. The data in **Figure V.C.1** shows that for an Isolink 4N49 there is a 30 to 40% decrease in the CTR when the device is warmed from room temperature (~23°C) to 100°C. Flight temperature conditions must be considered when assessing the performance of optocoupler in a space flight application.

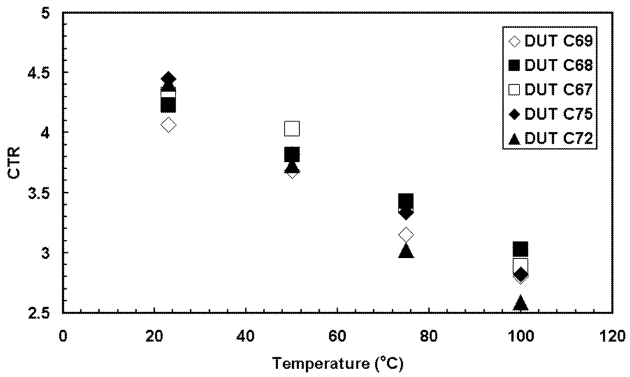

Figure V.C.1
Temperature effects on CTR for an Isolink 4N49 optocoupler [Reed-01].

Also, optocoupler reliability issues like LED aging effects must be considered when assessing on-orbit performance. In [John-00] it was shown that aging effects do not impact radiation-induced degradation characterization. However, the end-of-mission aging effects on LED must be considered when assessing optocoupler survivability.

VI. Optocoupler Down Select Based on Radiation Environment

VI.A Introduction

Optocoupler selection depends on the application and the shielded space radiation environment. In this section we will give guidance on how to select an optocoupler for certain space environments.

Figure VI.A.1 is a diagram showing the optocoupler down selection process. The analysis starts with an acceptable list of optocouplers based and electrical performance requirements. Followed by a down selection based on the radiation environment, optocoupler technology, and system requirements (we discuss this in more detail in the section below). The last phase of the down selection is radiation testing and analysis sequence for TID, DDD and SEEs. (These analyses were discussed in Section IV and Section V.) The order of this testing should be evaluated based on cost and risk. System considerations are an integral part of the assessment process. For single event effects, the Single Event Effects Criticality Assessment [SEECA] document should be used as a guide.

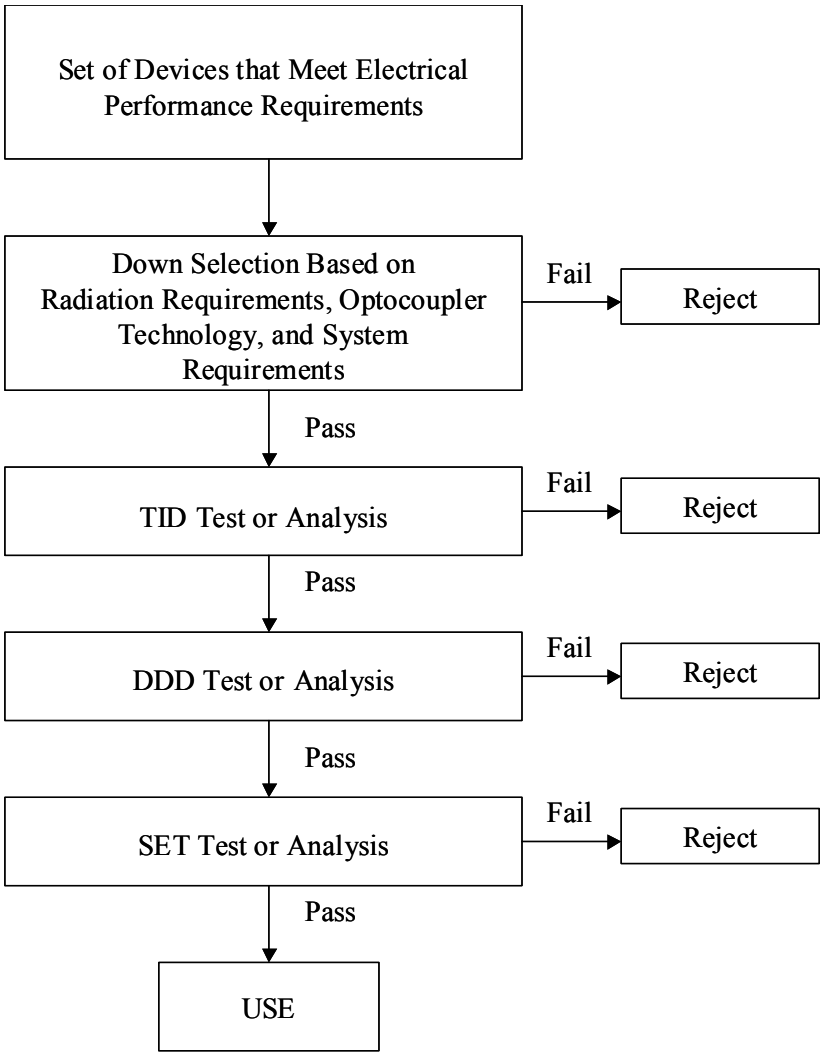

Figure VI.A.1
Process for down selecting optocouplers used in the space radiation environment.

VI.B Down Selection Based on Radiation Environment, Optocoupler Technology, and System Requirements

The recommended programmatic methodology that should be used to down select optocouplers is as follows (This is adapted from the general methodology for down selecting any microelectronic device [LaBe-98]):

1. define the hazard,
2. evaluate the hazard,
3. define requirements,
4. evaluate device usage,
5. "engineer" with designers,
6. iterate process as necessary.

A radiation effects expert that understands total ionizing dose, displacement damage and single event effects issues for optocouplers must perform this task. NASA Radiation Hardness Assurance (RHA) process recommends that a lead radiation effects engineer be assigned to all projects [LaBe-98].

VI.B.1 Define the Hazard

The first step of RHA in a program is to provide a "top-level" radiation environment definition based on parameters defined early in the mission. At this stage, the mission parameters will include orbit parameters, time of the launch and mission duration, and a nominal aluminum shield thickness. With this information, the radiation levels external to the spacecraft and behind nominal shielding are provided to the project as a top-level definition of the hazard. This definition includes contributions from trapped particles (protons and electrons), galactic cosmic ray heavy ions, and particles from solar events (protons and heavy ions). It should have the following components: 1) particle levels outside of spacecraft for trapped protons, electrons, and solar event protons to evaluate solar cell and surface damage, 2) particle levels inside spacecraft for "nominal" shielding for trapped protons, electrons, solar event protons to evaluate displacement damage and SEEs, 3) Linear-Energy-Transfer (LET) spectra inside spacecraft for galactic cosmic ray and solar heavy ions to evaluate SEEs, and 4) a total ionizing dose-depth curve for a generic geometry model (usually solid sphere). The dose depth curve should include contributions from trapped protons and electrons, solar event protons, and secondary bremsstrahlung. For SET analyses, the "shielded" particle levels should also include a definition of the normal background levels under which all systems must operate and the peak levels (SAA peak or peak during a solar event) for critical systems.

As the program matures, the lead radiation engineer must be informed of any changes to the mission parameters so he can evaluate the need to redefine the environment. Reducing design margins implies that small changes in mission parameters can cause the radiation requirement to go out of range of the design margin. For example, there are extremely large variations in the particle levels that a spacecraft encounters depending on its trajectory through the radiation sources. Also, the levels of all of the particle sources are affected by the activity cycle of the sun. Improvements to the solar cycle dependence of the newer models (e.g., CREME96 [Tylk-97] and Huston et al. [Hust-98]) mean that better estimates of variations in the environment due to the solar cycle are available. With this model capability, changes in launch dates can affect the environment definition.

VI.B.2 Evaluate the Hazard

After the hazard is defined, the effects that it will have on the systems are evaluated. The effects that are important to consider in RHA for optocouplers are long term damage from total ionizing dose and displacement damage and single event effects. The top-level environment definition provides adequate information to assess the level of hazard that the environment imposes and to identify the suitability of COTS for the program. There are no known sources for qualified radiation hardened optocouplers. If the project is does not accept the use of COTS then optocouplers will probably not be acceptable for critical systems.

VI.B.3 Define Requirements

A top-level radiation hazard is often used to derive mission requirements for most programs that are early in the design stage. This allows the radiation effects engineer to specify a requirement based on a nominal effective spacecraft shielding (such as 70 mills Al) using a generic geometry (such as solid sphere) before design details of the spacecraft are known. Performance requirements must be defined for all three of the major radiation effects issues: TID, displacement damage, and SEE. Several points must be kept in mind when defining requirements:

1) TID Radiation Design Margins (RDMs) of at least 2 should be included to cover uncertainties in the environment and device radiation hardness variances.

2) Different requirements may be set for different systems depending on system performance requirements, criticality level, shielding differences, etc.

3) Particle fluences (proton, electron, heavy ion, and neutron) need to be included for nominal, worst-case, and peak environments. For example, does the spacecraft need to gather science during a solar event (i.e., potential peak flux time period) or is a partial shutdown (safehold mode) acceptable?

4) Displacement damage requirements may be based on an external spacecraft environment such as "must survive an integral particle fluence of Y particles/cm^2 for E > X MeV protons". One must remember to pay special attention to non-ionizing energy loss (NIEL) and how it applies when the external particle spectrum is transported to an internal spacecraft environment. See Section V.B.3 for complete description.

5) SETs are perhaps the most complex issue. The GSFC radiation effects and analysis homepage [REA] includes a "generic" SEE specification for programs that allows for specifications to be set on a "system level". In particular, this specification covers analysis of event rates, system implications of the effects, and verification of mitigation techniques. One further note is the use of a single event effect criticality analysis (SEECA) to determine acceptable event rates also available on the GSFC homepage [SEECA]. The concept of this specification is to allow the use of non-SEE immune optocouplers by evaluating their usage and system mitigation schemes on a system level. This is a form of risk management.

VI.B.4 Evaluate Optocoupler Usage

The evaluation of device usage requires three processes: screening the list of optocouplers, radiation testing, and determining performance characteristics such as degradation or SET rates. Each of these areas is discussed below.

1. Screening: Once a list of optocouplers are received, the existing industry knowledge bases (RADATA, REDEX, GSFC test list, ERRIC, IEEE TNS and Data Workshop Records, etc.) are scanned for existing radiation data on each optocoupler type. The basic method for this data search and definition of usability is seen in the attached flow chart of **Figure VI.A.2**.

If data do not exist on the optocoupler, testing is required or a search for a device with similar non-radiation performance characteristics is undertaken.

2. Radiation Testing: Once a optocoupler list is reviewed versus archival data, devices must be identified for testing and the type of ground irradiations are decided on. We assign devices to three categories: high, medium, and low risk. Each of these are discussed in **Table VI.A.1**.

Table VI.A.1 Optocoupler Categories of Risk [LaBe-98]

High	those that have unknown radiation characteristics or previous lots with "suspect" radiation characteristics
Medium	those with some archival data or data from a "similar" optocoupler on the same process that indicates a potential issue but one that may be managed without extensive testing
Low	those that have lot-specific data or similar lots showing an excessive margin. This would include devices with sufficient test data or those where a previous lot's radiation characteristics excessively exceed the mission requirements

The type of testing depends on the type of device and mission requirements. As noted earlier, three specific areas are of concern (TID, displacement damage, and SEE). See Sections IV and V for a detail discussion on testing requirements.

The risk level can decrease if mitigation approaches are used. See Section VII for a description of mitigation approaches.

3. Determining Performance Characteristics: Once radiation test data have been obtained by test or from archival sources, the data must be applied to mission specific environment and application to determine device acceptability from the system level. See Sections IV and V for a detailed discussion on determining the performance characteristics.

It cannot be emphasized strongly enough that a test result is insufficient in determining device applicability without knowledge of the circuit, subsystems, and system effects.

VI.B.5 Engineer With Designers

On completion of the optocoupler usage evaluation, an engineering process with the spacecraft designers (and systems engineers) now occurs. For devices' whose predicted performance does not meet the mission requirements, alternative parts are now sought that may meet mission performance requirements (bandwidth, CTR, etc.) and have archival radiation data showing low or medium risk.

If such alternate components cannot be located, radiation mitigation methods (See Section VI.B) may be employed. For systems that fail to meet the mission total ionizing dose or the displace damage dose requirement defined by the top-level environment definition, it may be possible to redefine the hazard, especially if the requirement was set with a dose-depth curve. An effective approach is to utilize a spacecraft specific shielding definition to calculate total dose and particle levels at specific locations inside the spacecraft by using 3-D sectoring/ray trace and Monte Carlo techniques. By accurately defining the available shielding provided by spacecraft structures, boxes, boards, etc., the total dose and/or particle fluence requirement may be lowered.

Three-D radiation models are used almost exclusively for total ionizing dose and displacement damage dose evaluations, however, studies [Smit-94] have shown that single events effects rates on parts that are predominately proton-induced vary by a factor of two depending on the location within the spacecraft. This is not likely to be a concern for low earth orbits, but it may be more important as interest in the higher altitude regime grows where the proton environment is severe. Although it is well known that galactic cosmic ray heavy ions are barely affected by shielding, the attenuation of solar heavy ions is much greater. Careful evaluation of shielding may be important for systems that must operate through the peak of a solar event.

VI.B.6 Iterate Process

During the lifetime of a mission's design and development, multiple variables change. These include: updates to parts list, revised mechanical spacecraft layout, revised mission requirements such as mission duration, addition of new payloads, or the discovery of new radiation effects information.

Due to these and other factors, many of the steps in the approach may be revisited throughout a mission radiation effects program. Reevaluating TID and DDD requirements was discussed above. We recommend reviewing parts list at 6 month intervals.

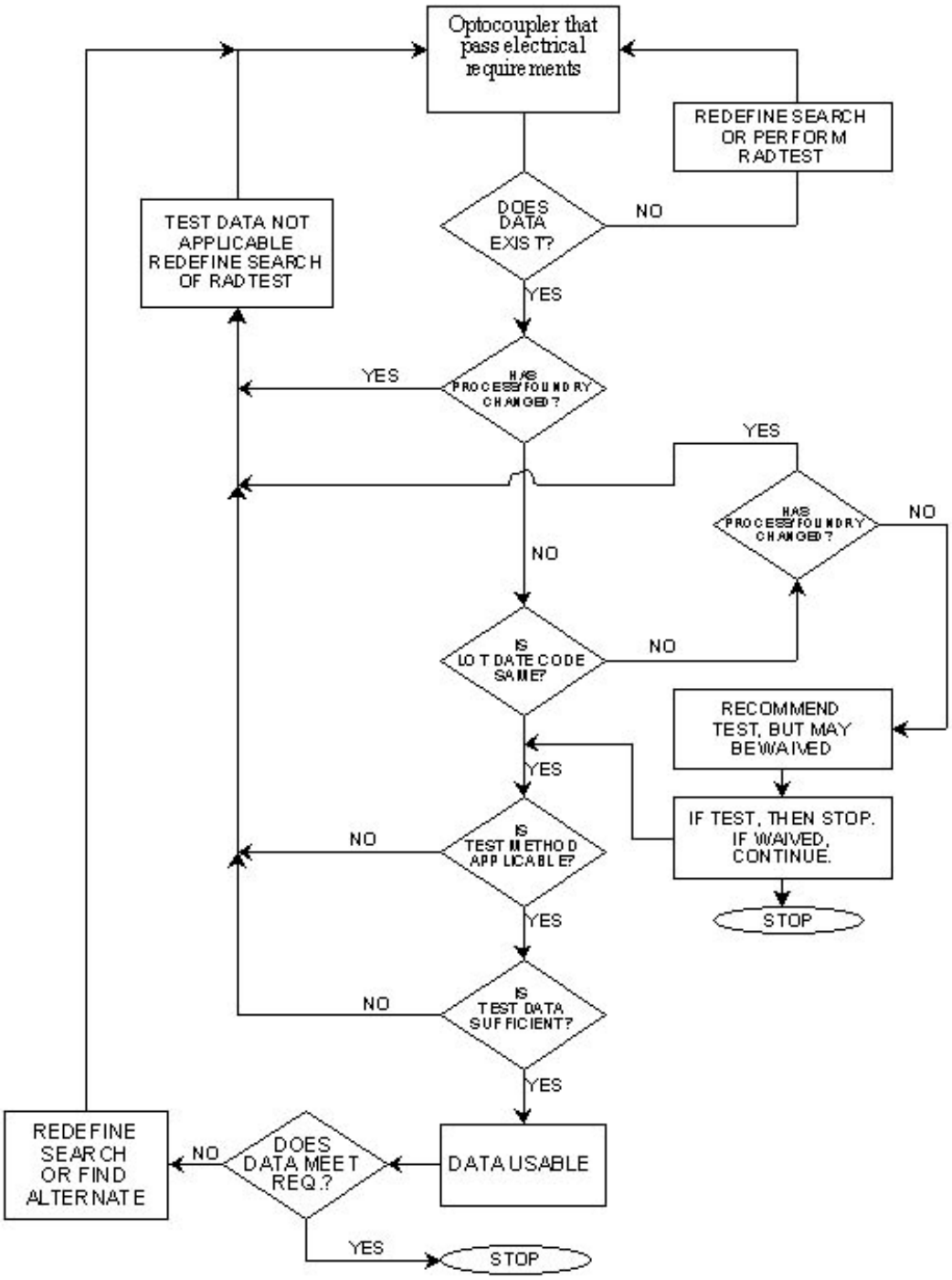

Figure VI.A.2
Basic method for data search and definition of part usability [LaBe-98].

VII. Mitigation Strategies

VII.A Introduction

Below is a series of recommendation on optocoupler mitigation strategies to reduce the risk of radiation-induced performance degradation. We cover items like optocoupler components selection, simple application modifications, and on-orbit procedures. Several concepts described early in Sections I through VI will be summarized in this section, we refer the reader to these sections for the references to these concepts.

The first two are related to mitigation of SETs and the others are related to mitigating the effects of TID and DDD.

VII.B Photodetector Selection

The susceptibility of photodetectors to direct-ionizing proton SETs demonstrates the importance of minimizing the volume in which the detectors are susceptible to ion-generated photocurrents. This criterion can be extremely important in selecting components that may perform acceptably in space radiation environments. Direct-bandgap semiconductors, such as GaAs and InGaAs, require much thinner intrinsic semiconductor layers than do indirect-bandgap semiconductors, such as Si and Ge. As a result, direct-bandgap devices are less susceptible to SETs [Mars-94b]. However, to date there are no optocoupler manufactures that utilize indirect-bandgap photodiodes.

VII.C Filtering SET

The effects of using an RC network at the output a high speed digtal signal isolater was discuss in Section IB.B (See **Table IV.B.1).** The resulting RC network suppresses the transient propagation to other circuit elements. RC network can be used with either current transfer or high speed digital signal isolators to mitigate the transient but it compromises the circuit bandwidth, which in some applications may be unacceptable.

VII.D Optocoupler-LED Selection

DDD is the main concern for LED selection. Amphoterically doped and single heterojunction LED degrade at a much high rate than double heterojunction LEDs. For identical output application conditions an optocoupler that uses a double heterojunction LED will survive longer than the other two technologies.

In [John-00], the authors suggest that even though amphoterically doped LEDs degrade at a faster rate, one might select these over the double heterojunction devices. This is because the light output of an amphoterically doped LED could be greater than that for the double heterojunction junction LED at the same drive current for the equivalent displacement damage dose. Choosing to use an amphoterically doped LED over a double heterojunction device requires one to have a higher degree of confidence in the accuracy degradation prediction techniques.

TID effects on LED performance is typically a second order effect for current LED technology and for the typical mission with dose (<0.5Mrad(Si)). SETs are not a concern for current technology.

VII.E Increased Drive Current

The mitigation technique described next can be used for current transfer device applications. Increasing the LED drive current cause the LED to emit more optical power. Increasing the LED drive current will compensate for the radiation-induced optical power output.

The results from exposing six P2824 Hamamatsu with a 51.8 MeV proton beam at Loma Linda University Medical Center are shown in **Figure VII.C.1.** This figure plots the average CTR as a function on drive current for various fluence levels. The legend shows the fluence levels. The error bars show the spread in the CTR for the devices tested.

These data show that increasing drive current can significant mitigate the effects radiation. However, increasing the drive current can lead to early failure of the optocoupler due to wearout of the LED. A reliability expert should be consulted.

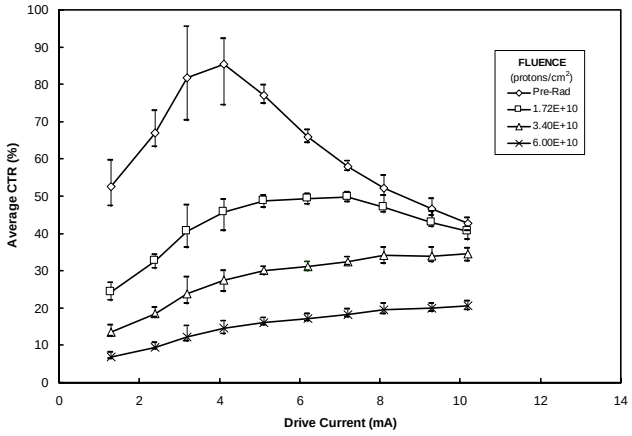

Figure VII.C.1
Average percent CTR for various drive currents.

VII.F Collector-Emitter Voltage

The mitigation technique described next can be used for current transfer device applications. Reduced light output due to radiation is, in effect, reducing the base current of the collect (Section V.B.3). If the base current is changed when operating in the active region then the optocoupler I_C will change. However, if the base current is changed while the device is in saturation, the collector current (I_C), and hence the CTR, will remain essentially constant. Using the optocoupler in a way that the collector current is saturated allows for a more stable optocoupler output. However, it does increase the on orbit lifetime of the optocoupler.

VII.G Intra-Lot Optocoupler Selection for Current Transfer Device Applications

The mitigation technique described next can be used for current transfer device applications. Proper intra-lot optocoupler selection can allow for more CTR margin. **Figure VII.C.2** shows the percent of the optocouplers that have a certain CTR for the Isolink 4N49. These data where taken at a drive current of 8 mA. Note that there is a distribution of CTR values. Selecting a device that has an initially larger CTR can give more than a factor of two more margin in the CTR.

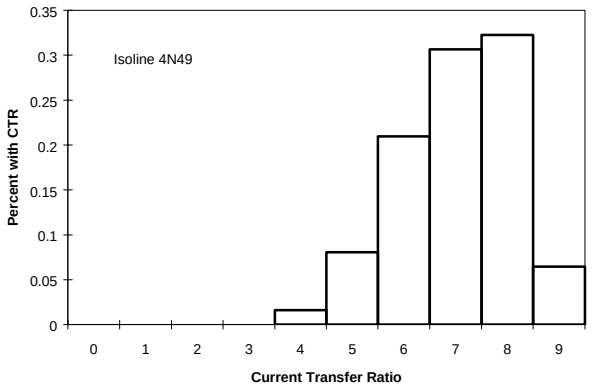

VII.H Annealing considerations

Injection current annealing of displacement damage-induced degradation of optocoupler CTR was summarized in Section V.B.3. However, an accelerated annealing test has not been developed as of yet. The effects of anneal should not be considered a mitigation approach, even though there will be some recovery for application with higher currents.

I. References

[1019.5] 1019.5

[Barr-95] A.L. Barry, et al., "The Energy Dependence of Lifetime Damage Constants in GaAs LEDs for 1-500MeV Protons," IEEE Trans. Nuc. Sci., 42(6), December 1995: 2104-2107.

[Barn-84] C.E. Barnes and J.J. Wiczer, "Radiation effects in optoelectronic devices," Sandia Report, SAND84-0771, 1984.

[Barn-86] C.E. Barnes, "Radiation hardened optoelectronic components: sources," Proc. SPIE, vol. 616, pp. 248-252, 1986.

[Bart-97] J. Barth, "Modeling space radiation environments," Notes from 1997 IEEE Nuclear and Space Radiation Effects Conference Short Course.

[Burk-87] E.A. Burke, C.J. Dale, A.B. Campbell, G.P. Summers, T. Palmer, and R. Zuleeg, "Energy Dependence of Proton-Induced Displacement Damage in GaAs, IEEE Tranc. Nucl. Sci., Vol. 34, No. 6, p. 1220, 1987.

[D'Odi-97] M. D'Ordine, "Proton Displacement Damage in Optocouplers." IEEE Radiation Effects Data Workshop, July 1997: 122-124.

[Dres-98] P. V. Dressendorfer, "Basic mechanisms for the new millenium," Notes from 1998 IEEE Nuclear and Space Radiation Effects Conference Short Course.

[Epst-72] A.S. Epstein, P.A. Trimmer. "Radiation Damage and Annealing Effects in Photon Coupled Isolators." IEEE Trans. Nuc. Sci., 19(6), December 1972: 391-399.

[F1192] ASTM Web Site.

[Hust-98] S.L. Huston, and K.A. Pfitzer, "A New Model for the Low Altitute Trapped Proton Environment," accepted for publication at IEEE Nuclear Science and Radiation Effects Conference, Jul. 1998.

[JEDEC HI] JEDEC Heavy Ion Test Document.

[John-98] A.H. Johnston, et al., "Single-Event Upset Effects in Optocouplers." IEEE Trans. Nuc. Sci., 45(6), December 1998: 2867-2875.

[John-99a] A.H. Johnston, B.G. Rax, L.E. Selva, C.E. Barnes, "Proton degradation of light-emitting diodes," IEEE Trans. Nucl. Sci. vol. NS-46, pp. 1781-1789, 1999

[John-99b] A.H. Johnston, T. Miyahira, G.M. Swift, S.M. Guertin, L.D. Edmonds, "Angular and energy dependence of proton upset in optocouplers," IEEE Trans. Nucl. Sci. vol. NS-46, pp. 1335-1341, 1999

[John-00] Allan Johnstons short course in 2000.

[LaBe-97] K.A. LaBel, P.W. Marshall, C.J. Marshall, M. D'Ordine, M. Carts, G. Lum, H.S. Kim, C.M. Seidleck, T. Powell, R. Abbott, J. Barth, E.G. Stassinopoulos, "Proton-induced transients in optocouplers: in-flight anomalies, ground irradiation test, mitigation and implications," IEEE Trans. Nucl. Sci. vol. NS-44, pp. 1885-1892, 1997.

[LaBe-98] K.A. LaBel, et a.RHA paper

[LaBe-00] Ken LaBel et al., "A Compendium of Recent Optocoupler Radiation Test Data," IEEE Radiation Effects Data Workshop, July 2000: 123-146.

[Lera-99] J.L. Leray, "Total dose effects: modeling for the present and future," Notes from 1999 IEEE Nuclear and Space Radiation Effects Conference Short Course.

[Mars-92] P.W. Marshall, C.J. Dale, and E.A. Burke, "Space radiation effects on optoelectronic materials and components for a 1300 nm fiber optic data bus," IEEE Trans. Nucl. Sci., vol. 39, no. 6, pp. 1982-1989, 1992.

[Mars-94b] P.W. Marshall, C.J. Dale, E.J. Friebele, and K.A. LaBel, "Survivable fiber-based data links for satellite radiation environments," SPIE Critical Review CR-14, Fiber Optics Reliability and Testing, pp. 189-231, 1994.

[Mars-99] P.W. Marshall, and C.J. Marshall, "Proton Effects and Test Issues for Satellite Applications," IEEE NSREC99 Short Course, IV1-110, July 1999.

[MG] SET Prediction Tool for Protons.

[p+ LL] Lessons Learned Document for Proton Testing.

[Rax-96] B.G, Rax, et al., "Total Dose and Proton Damage in Optocouplers." IEEE Trans. Nuc. Sci., 43(6), December 1996: 3167-3173.

[REA] NASA/GSFC Radiation Effects and Analysis home page http://flick.gsfc.nasa.gov/radhome.htm.

[Reed-98] R.A Reed, P.W. Marshall, A.H. Johnston, J.L. Barth, C.J. Marshall, K.A. LaBel, M. D'Ordine, H.S. Kim, M.A. Carts, "Emerging Optocoupler Issues With Energetic Particle-Induced Transients And Permanent Radiation Degradation," IEEE Trans. Nucl. Sci. vol. NS-45, pp. 2833 –2841, 1998.

[Reed-00] R.A. Reed, P.W. Marshall, C.J. Marshall, R.L. Ladbury, H.S. Kim, L.X. Nguyen, J.L. Barth, and K.A. LaBel, "Energy Dependence of Proton Damage in AlGaAs Light Emitting Diodes," IEEE Trans. Nuc. Sci., 47(6), December 2000: 2492-2499.

[Reed-01] TNS 2001 Opto Paper.

[SEECA] GSFC Single Event Effects Criticality Assessment (SEECA) Document.

[Smit-94] Ed Smith "Effects of Realistic Satellite Shielding on SEE Rates," IEEE Trans. on Nuclear Science, vol 41, no. 6, pp. 0018-9499, Dec. 1994.

[Soda-75] K.J. Soda, et al. "The Effect of Gamma Irradiation on Optical Isolators," IEEE Trans. Nuc. Sci., 22(6), December 1975: 2475-2481.

[Summ-88] G.P. Summers, E.A. Burke, M.A. Xapsos, C.J. Dale, P.W. Marshall, and E. Petersen, "Displacement damage in GaAs structures, " IEEE Trans. Nucl. Sci., Vol. 35, No. 6, 1988

[Tylk-97] A.J. Tylka, J.A. Adams, Jr., P.R. Boberg, B.Brownstein, W.F. Dietrich, E.O. Flueckiger, E.L. Petersen, M.A. Shea, D.F. Smart, and E.C. Smith, "CREME96: A Revision of the Cosmic Ray Effects on Micro-Electronics Code," IEEE Trans. on Nuclear Science, vol 44, no. 6, pp. 0018-9499, Dec. 1997.

[Wicz-86] J.J. Wiczer, "Radiation hardened optoelectronic components: Detectors," Proc. SPIE, vol. 616, pp. 254-266, 1986.

[Zieg-84] J.F. Ziegler, J.P. Biersack, and U. Littmark, The Stopping and Range of Ions in Solids. New York: Pergamgon, 1884.